

AD-A133 526

EFFECT OF RADIOFREQUENCY RADIATION ON DNA DUPLEX
STABILITY AND REPLICATION(U) MISSOURI UNIV-ROLLA
R F BROWN ET AL. AUG 83 USAFSAM-TR-83-20

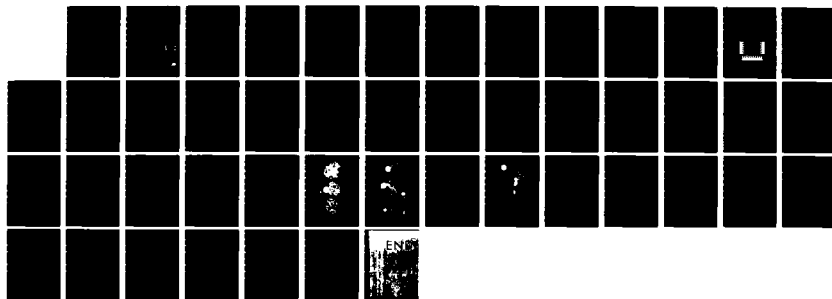
1/1

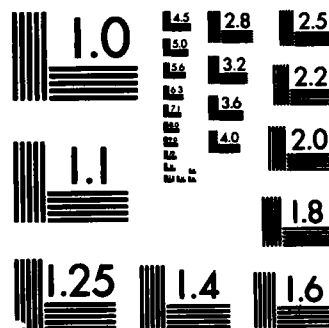
UNCLASSIFIED

F33615-80-C-0613

F/G 6/18

NL





MICROCOPY RESOLUTION TEST CHART
NATIONAL BUREAU OF STANDARDS-1963-A

12

AD-A133526

EFFECT OF RADIOFREQUENCY RADIATION ON DNA DUPLEX STABILITY AND REPLICATION

Roger F. Brown, Ph.D.
Stanley V. Marshall, Ph.D.

Life Sciences and Electrical Engineering Departments
University of Missouri-Rolla
Rolla, Missouri 65401

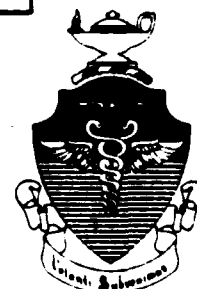
DTIC
ELECTE
OCT 13 1983
B

August 1983

Final Report for Period 30 April 1981 - 30 November 1982

Approved for public release; distribution unlimited.

Prepared for
USAF SCHOOL OF AEROSPACE MEDICINE
Aerospace Medical Division (AFSC)
Brooks Air Force Base, Texas 78235



DUPLICATE COPY

83 10 11 032

NOTICES

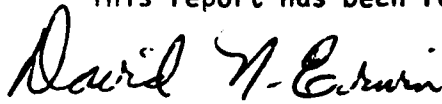
This final report was submitted by the University of Missouri-Rolla, Departments of Life Sciences and Electrical Engineering, Rolla, Missouri 65401, under contract F33615-80-C-0613, job order 7757-01-84, with the USAF School of Aerospace Medicine, Aerospace Medical Division, AFSC, Brooks Air Force Base, Texas. Dr. David N. Erwin (USAFSAM/RZP) was the Laboratory Project Scientist-in-Charge.

When Government drawings, specifications, or other data are used for any purpose other than in connection with a definitely Government-related procurement, the United States Government incurs no responsibility or any obligation whatsoever. The fact that the Government may have formulated or in any way supplied the said drawings, specifications, or other data, is not to be regarded by implication, or otherwise in any manner construed, as licensing the holder, or any other person or corporation; or as conveying any rights or permission to manufacture, use, or sell any patented invention that may in any way be related thereto.


The animals involved in this study were procured, maintained, and used in accordance with the Animal Welfare Act and the "Guide for the Care and Use of Laboratory Animals" prepared by the Institute of Laboratory Animal Resources - National Research Council.

The Office of Public Affairs has reviewed this report, and it is releasable to the National Technical Information Service, where it will be available to the general public, including foreign nationals.

This report has been reviewed and is approved for publication.


DAVID N. ERWIN, Ph.D.
Project Scientist


JOHN C. MITCHELL, B.S.
Supervisor


ROYCE MOSER, Jr.
Colonel, USAF, MC
Commander

UNCLASSIFIED

SECURITY CLASSIFICATION OF THIS PAGE (When Data Entered)

REPORT DOCUMENTATION PAGE		READ INSTRUCTIONS BEFORE COMPLETING FORM
1. REPORT NUMBER USAFSAM-TR-83-20	2. GOVT ACCESSION NO.	3. RECIPIENT'S CATALOG NUMBER
4. TITLE (and Subtitle) EFFECT OF RADIOFREQUENCY RADIATION ON DNA DUPLEX STABILITY AND REPLICATION		5. TYPE OF REPORT & PERIOD COVERED Final Report 30 Apr 1981-30 Nov 1982
		6. PERFORMING ORG. REPORT NUMBER
7. AUTHOR(s) Roger F. Brown, Ph.D. Stanley V. Marshall, Ph.D.		8. CONTRACT OR GRANT NUMBER(s) F33615-80-C-0613
9. PERFORMING ORGANIZATION NAME AND ADDRESS Life Sciences and Electrical Engineering Depts. University of Missouri-Rolla Rolla, Missouri 65401		10. PROGRAM ELEMENT, PROJECT, TASK AREA & WORK UNIT NUMBERS 62202-F 7757-01-84
11. CONTROLLING OFFICE NAME AND ADDRESS USAF School of Aerospace Medicine (RZP) Aerospace Medical Division (AFSC) Brooks Air Force Base, Texas 78235		12. REPORT DATE August 1983
		13. NUMBER OF PAGES 42
14. MONITORING AGENCY NAME & ADDRESS (if different from Controlling Office)		15. SECURITY CLASS. (of this report) Unclassified
		15a. DECLASSIFICATION/DOWNGRADING SCHEDULE
16. DISTRIBUTION STATEMENT (of this Report) Approved for public release; distribution unlimited.		
17. DISTRIBUTION STATEMENT (of the abstract entered in Block 20, if different from Report)		
18. SUPPLEMENTARY NOTES		
19. KEY WORDS (Continue on reverse side if necessary and identify by block number) Radiofrequency radiation DNA replication in vivo Sister chromatid exchange DNA degradation Mice		
20. ABSTRACT (Continue on reverse side if necessary and identify by block number) <p>➤ Three experimental approaches were used to determine if absorption of continuous wave radiofrequency (RF) photons affect the stability and/or replication of mammalian DNA. Two of the approaches involved experiments with female CD-1 mice, including analyses of RF effects on sister chromatid exchanges (SCE) in bone marrow as one index of DNA stability and RF effects on replication of the animals' marrow and spleen DNA. The third</p> <p style="text-align: right;">(over)</p>		

UNCLASSIFIED

SECURITY CLASSIFICATION OF THIS PAGE (When Data Entered)

UNCLASSIFIED

SECURITY CLASSIFICATION OF THIS PAGE(When Data Entered)

20. ABSTRACT (Continued)

experimental approach consisted of tests to determine if RF exposure causes partial denaturation of double-stranded DNA, monitored in this study by susceptibility of the polymer to hydrolysis by single-strand-specific S₁ nuclease. The substrate DNA used for this cell-free assay was isolated from Chinese hamster ovary cell cultures labeled with radioactive deoxynucleosides. Irradiated subjects were exposed to incident RF field densities adjusted to be equivalent to absorbed doses in mice of 4 W/kg at each of three test frequencies: 400, 800, and 1200 MHz. A transverse-electromagnetic-mode chamber was used for 400-MHz exposures, and two small anechoic chambers were used at 800 and 1200 MHz. Predetermined adjustments of the temperature of ventilating air forced through the chambers permitted maintenance of the core temperature of the RF-irradiated animals at the same level as that of the sham-exposed controls. The results revealed no reduction in the level of DNA synthesis in either the spleen or the bone marrow of animals exposed to any of the three test frequencies, also no increase in the number of SCE. However, a slight, but consistent, increase in the nuclease susceptibility of isolated DNA appeared to be a result of RFR exposure. This effect was observed at all three of the irradiation frequencies.

Accession For	
NTIS GRA&I	<input checked="checked" type="checkbox"/>
DTIC TAB	<input type="checkbox"/>
Unannounced	<input type="checkbox"/>
Justification	
By	
Distribution/	
Availability Codes	
Dist	Avail and/or Special
A	



UNCLASSIFIED

SECURITY CLASSIFICATION OF THIS PAGE (When Data Entered)

TABLE OF CONTENTS

	<u>Page</u>
INTRODUCTION	3
EXPOSURE DEVICES AND INSTRUMENTATION	4
Radiofrequency Exposure and Ventilation Systems	4
Instrumentation	8
TECHNICAL APPROACH	9
Animals	9
Chemicals	9
SAR and Power Density Measurements	9
Core Temperature Measurements	11
Intravenous Infusion	11
DNA Synthesis Measurement	12
Sister Chromatid Exchange Analysis in Vivo	13
S ₁ Nuclease Assay	14
RESULTS AND DISCUSSION	15
Power Density and Field Uniformity	15
SAR Measurements	15
Airflow through TEM and Anechoic Chambers	21
Core Temperature: RFR Subjects	21
Sister Chromatid Exchange: RFR Effects	27
DNA Synthesis: RFR Subjects	34
S ₁ Hydrolysis of DNA: RFR Effects	36
CONCLUSIONS	40
ACKNOWLEDGMENTS	40
REFERENCES	41

List of Figures and Tables

Figure

1	TEM chamber system for RF exposures at 400 MHz	5
2	Anechoic chamber system for RF exposures at 800 and 1200 MHz	6
3	Interior of anechoic chambers	7
4	Protocol for injecting radioactive precursors to label DNA in the spleen and marrow tissue of mice	12
5	Protocol for administering BrdUrd and colcemid to mice for SCE analysis in marrow tissue	13

<u>Figure</u>		<u>Page</u>
6	Ratios of measured power-density values to calculated power-density values for the anechoic chambers	16
7	Power densities along the work surface of the large-horn anechoic chamber	17
8	Power densities along the work surface of the small-horn anechoic chamber	18
9	SAR values measured for mouse cadavers exposed to 600-1200 MHz . .	19
10	Change in colonic temperature of mice exposed to 400 MHz	23
11	Colonic temperature of irradiated mice adjusted by air-temperature variation	24
12	Change in colonic temperature of mice exposed to 800 and 1200 MHz	25
13	Colonic temperatures of mice exposed to different temperatures of forced airflow ventilating the anechoic chambers	26
14	Appearance of fluorescent-plus-Giemsa-stained metaphase chromosomes from the bone marrow of mice	28
15	Differentially stained second-division-cycle marrow chromosomes from mice treated with different concentrations of cyclophosphamide	29
16	Differentially stained second-division-cycle marrow chromosomes from sham- and RF-irradiated mice	31

<u>Table</u>		
1	Cyclophosphamide induction of SCE in bone marrow of mice	30
2	Number of SCE observed in marrow chromosomes of RFR- and sham-exposed mice	32
3	Mean comparisons of SCE frequencies in marrow cells of RFR- and sham-exposed mice	33
4	Effect of hydroxyurea on formation of spleen DNA in vivo: $^3\text{H}/^{14}\text{C}$ ratios used to assess relative levels of DNA synthesis . .	34
5	Relative levels of DNA synthesis in sham- and RFR-exposed mice . .	35
6	Test of DNA type used as substrate for S_1 hydrolysis	37
7	Effect of RFR exposure on hydrolysis of ^3H -DNA by S_1 nuclease . .	39

EFFECT OF RADIOFREQUENCY RADIATION ON DNA DUPLEX STABILITY AND REPLICATION

INTRODUCTION

Results of recent theoretical analyses by Prohofsky and colleagues (Kohli et al., 1981; Mei et al., 1981) indicate that RFR absorption by double-stranded DNA excites various vibrational responses in the macromolecule, including bending, torsion, and compression. These investigators have particularly focused on vibration and hydrogen-bond stretching near free ends in the strands. The level of RFR theoretically absorbed by a synthetic polydeoxynucleotide, double-helical poly dG-poly dC, appears sufficient to induce melting of hydrogen bonds between the complementary bases of five nucleotide pairs bordering the termini (Putnam et al., 1981). This partial separation of strands at free ends is also thought to be frequency specific, possibly occurring in the 750- to 900-MHz range (E. Prohofsky, personal communication, 1981).

To assess the likelihood of RFR-induced strand separation at free ends by a mechanism such as that proposed by Prohofsky and colleagues, we must, in part, consider the nature of eukaryotic chromosomes. There is evidence of no gaps or free ends in G_0 cells. Electron micrographs reveal chromosome-to-chromosome connections in human metaphase cells, suggesting that nuclear DNA may be a continuum (Lampert et al., 1969). Also, the DNA of G_0 cells is resistant to hydrolysis by S_1 nuclease, an enzyme that acts at gap regions (Collins, 1977). However, replicating chromosomes have numerous free ends as evidenced both by susceptibility to S_1 nuclease (Collins, 1977) and by the formation of Okazaki fragments that are subsequently joined by a ligase (Huberman and Horwitz, 1973). Free ends are also present during excision and repair of damaged segments (Hanawalt et al., 1979). DNA undergoing replication, repair, or recombination would seem, therefore, the most likely target for the hypothetical RFR-induced denaturation of termini.

From a biologic point of view, destabilization of DNA termini by RFR-enhanced vibration would be potentially hazardous. The purpose of this investigation was to search for evidence of frequency-specific RFR effects on the replication and stability of mammalian DNA. Three different approaches were used to experimentally test for DNA perturbations at frequencies of 400, 800, and 1200 MHz continuous wave (CW). Two of the approaches involved *in vivo* tests with mice, and the third was a direct test for RFR-induced denaturation of isolated duplex DNA.

The first approach in this investigation focused on RFR induction of sister chromatid exchange (SCE) as an indirect test for strand separation. The rationale behind this approach was that an increased number of recombination events, including SCE, would be predicted if RFR exposure causes DNA strands to partially denature at free ends. This would be manifested as an increased frequency of SCE in the marrow cells of the irradiated animals.

The second approach involved analysis of RFR effects on DNA replication in dividing cells; specifically, the bone marrow tissue and spleen of intact mice.

The reasoning behind this portion of the investigation was that any RFR-induced denaturation at growing points in replicating DNA would impede elongation of the segments of nascent DNA, resulting in a decrease in total DNA synthesis. Indeed, exposure to 1000-MHz waves has been reported to partially inhibit DNA replication in murine leukemia cells (Chang et al., 1980).

The third approach was to look for direct interaction of RFR with DNA, resulting in enhanced hydrolysis of the macromolecule by S_1 nuclease. RFR-induced denaturation of duplex DNA at exposed ends should render these single-stranded regions susceptible to the action of S_1 nuclease, an enzyme that hydrolyzes single-stranded DNA to 5'-mononucleotides but does not degrade double-stranded DNA (Ando, 1966; Vogt, 1973). This enzymatic degradation was monitored as release of acid-soluble radioactivity from 3H -labeled duplex DNA exposed to RFR during incubation with S_1 nuclease.

An existing transverse-electromagnetic-mode (TEM) exposure chamber was used for RF irradiation of mice at 400 MHz. Two specially constructed anechoic chambers were used for the RF exposures at 800 and 1200 MHz. Incident RF power densities were adjusted at each of the three test frequencies to be equivalent to absorbed doses of 4 W/kg for mice. Air maintained at predetermined temperatures was forced through the sham and RF enclosures to align the core temperatures of the irradiated animals to essentially the same level as that recorded for the sham-exposed control subjects. RF-irradiated capillary tubes containing the DNA- S_1 nuclease reaction mixtures were subjected to the same incident power densities used for the animal exposures, with air temperatures adjusted to the same level as that for control reactions--37.4°C.

An underlying requirement of this investigation was uniform power density of the RF field for animal exposures. This requirement limited the practical number of mice that could be positioned simultaneously in our anechoic chambers to four. Hence, each replication was designed to include four RFR-exposed and four sham-exposed mice. RFR exposures were with the subjects oriented parallel to the E-field.

EXPOSURE DEVICES AND INSTRUMENTATION

Radiofrequency Exposure and Ventilation Systems

Two different irradiation systems were used for RFR exposures in this investigation. One was built around a TEM chamber (model 8801, Narda) and was used for exposures in the 200- to 475-MHz range. The second included two specially constructed anechoic chambers used for exposures in the 600- to 1200-MHz range. The 200- to 475-MHz system (Fig. 1) has been described in detail previously (Brown et al., 1981).

The 600- to 1200-MHz exposure system (Fig. 2) included small anechoic chambers constructed as two identical 1.22- x 1.22- x 1.22-m plywood boxes lined with microwave absorbant material (type AAP-12, Advanced Absorber Products) as shown in Figure 3. The corners of the enclosures were filled with 20-cm-thick absorbant material (not shown in Fig. 3) to reduce RF leakage.

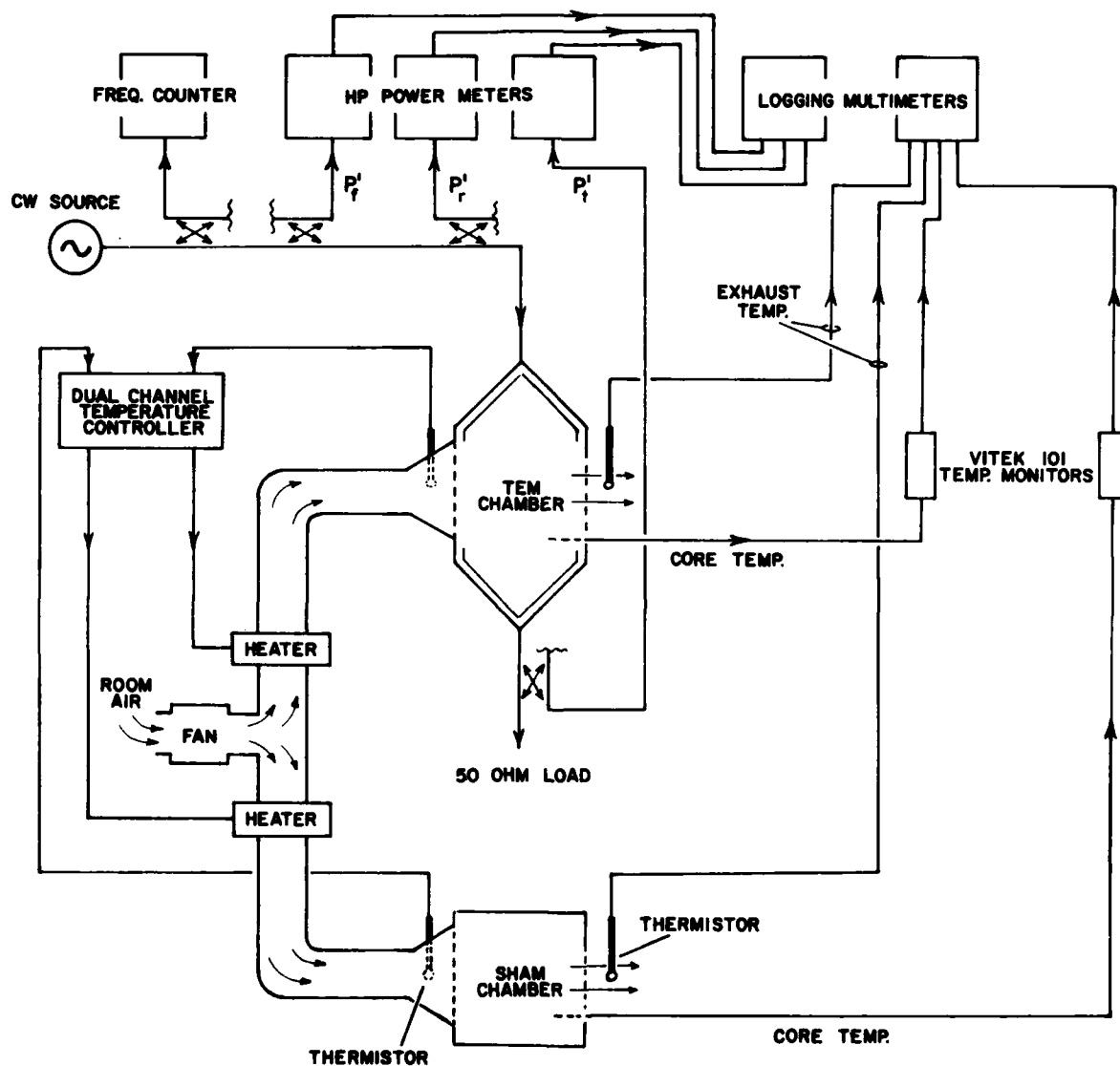


Figure 1. TEM chamber system for RF exposures at 400 MHz. Components for controlled-temperature ventilation are also illustrated.

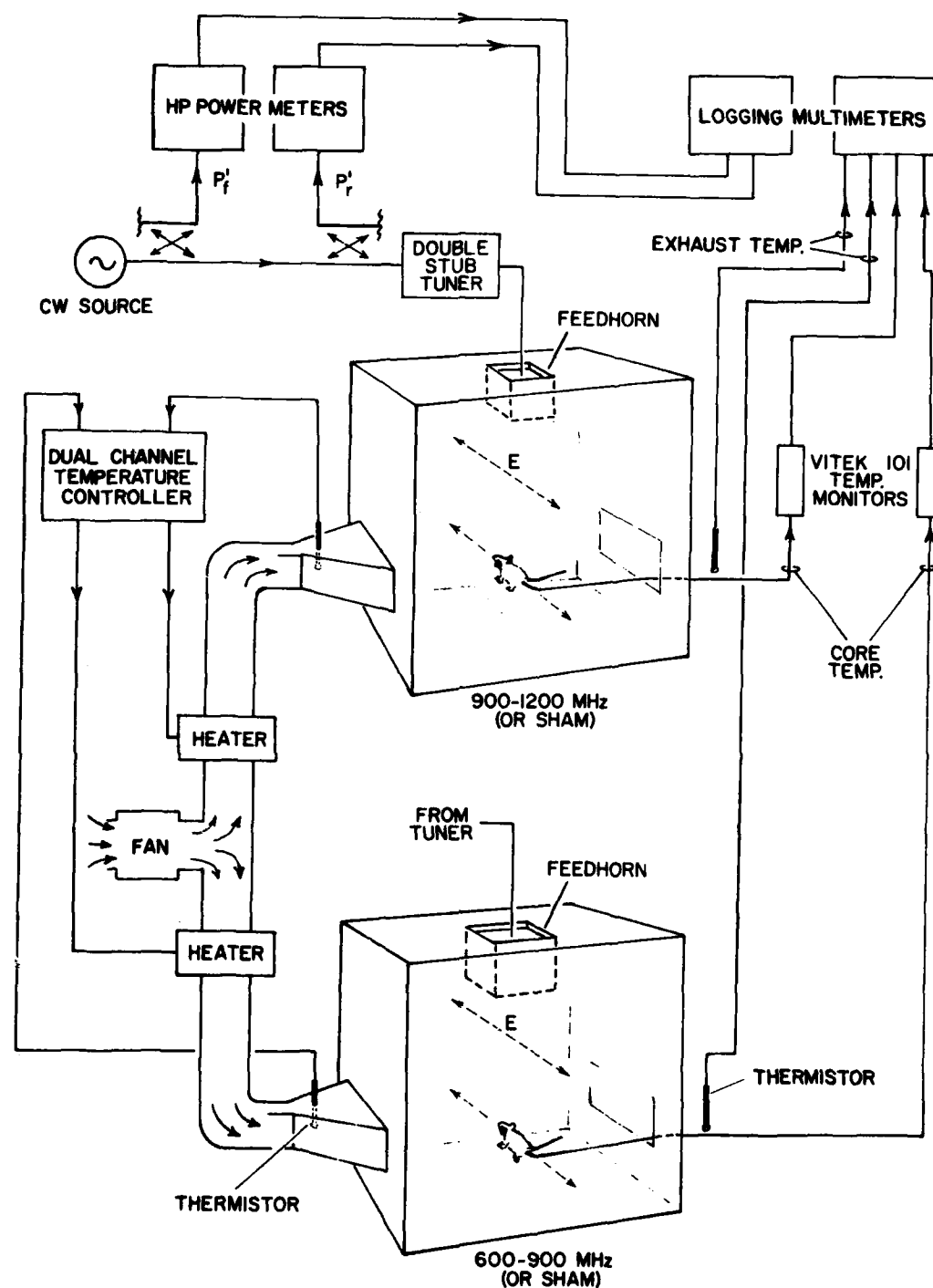


Figure 2. Anechoic chamber system for RF exposures at 800 and 1200 MHz. Components for control and temperature ventilation are also illustrated.

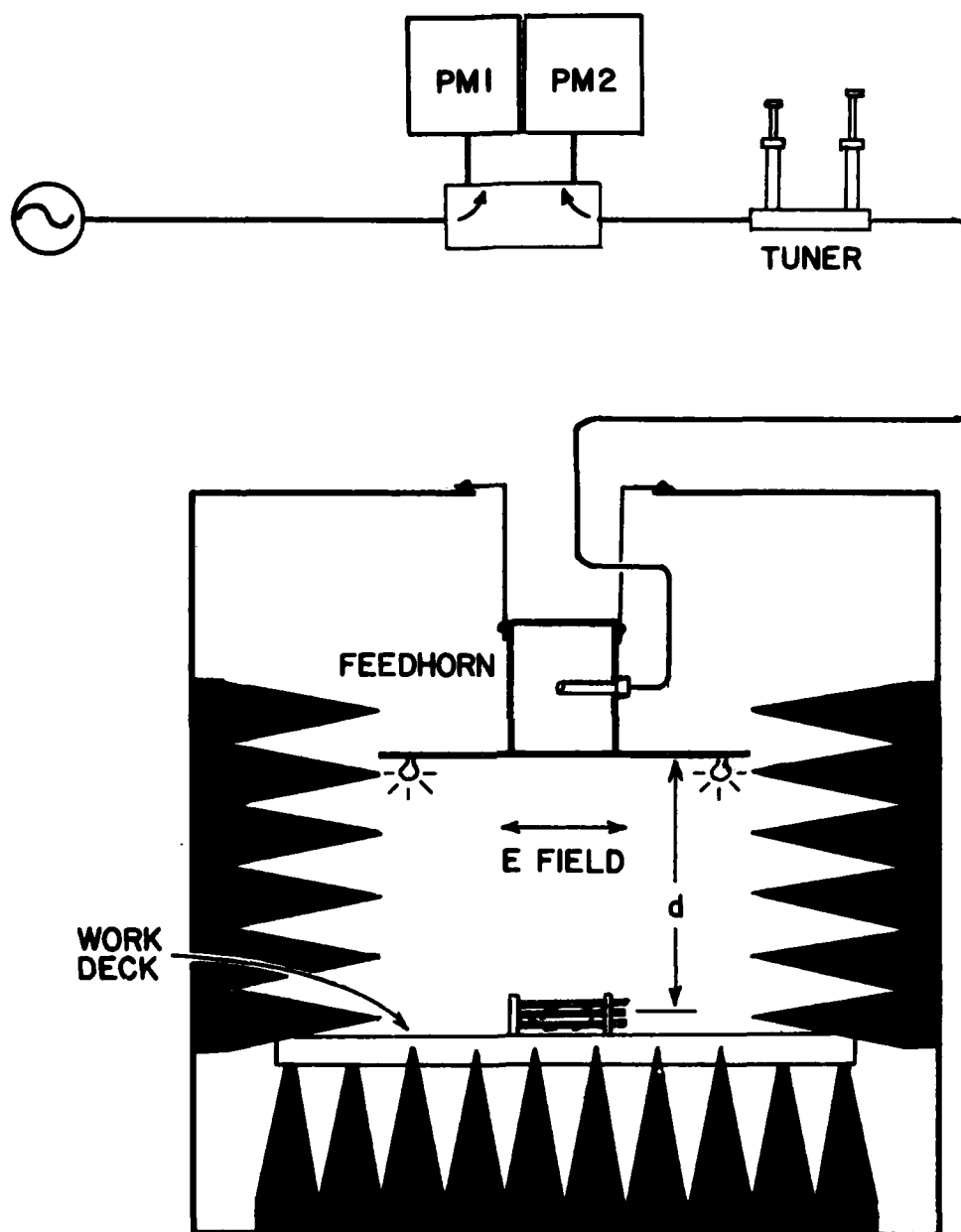


Figure 3. Interior of anechoic chambers. Power meters PM1 and PM2 monitor forward and reflected power respectively. Distance d is 43 cm.

A feedhorn, a coax-waveguide adapter, was at the top of each chamber. In both chambers the aperture of the feedhorn was positioned 84 cm above the plywood floor and 45 cm above a Styrofoam work deck (Fig. 3), the subject-exposure surface. One of the anechoic chambers was equipped with a 33.65- x 17.15-cm-aperture horn for 600- to 900-MHz irradiation, and the other with a 22.45- x 11.43-cm-aperture horn for 900- to 1200-MHz operation. The aperture of each horn, oriented downward, was covered with a 61- x 61-cm masonite panel such that, from the Styrofoam deck, both horns appeared identical. When the chamber with the larger horn was used for irradiation in the 600- to 900-MHz range, the second chamber served as a sham enclosure; for 900- to 1200-MHz operation, the roles were reversed. Lighting in each chamber was provided by two 15-W bulbs mounted on the masonite panel on either side of the irradiating horn (Fig. 3).

Removable access ports, lined with absorbant material, permitted entry from the side of each chamber. The integrity of the absorbant surface was maintained when the plugs were in place.

The anechoic chambers were ventilated by forced airflow (see Fig. 2). A single blower forced room air through both an RFR exposure chamber and its corresponding sham enclosure. The ventilation system was designed to be easily connected to either the TEM exposure system or the anechoic chambers. A small (25 x 7.6 cm) rectangular opening for inflow air was in one wall of the anechoic chambers; an opening of similar size for exhaust air was in the opposite wall. Inflow air, directed to the work surface via a rectangular cardboard channel (25 x 7.6 cm, cross section), was tuned such that the volume of air flowing across the area of the work deck occupied by the test subject was nearly uniform (within about $\pm 10\%$).

The ventilating air was forced through a preheater that warmed it to about 26°C. The preheated air was split by a T-connector, passed through two separately controlled heaters, and directed via flexible hose to the inflow port of each chamber (Figs. 1 and 2). A thermistor mounted on the exhaust port for each chamber monitored the exhaust air temperature. A feedback thermistor, the sensing element for the temperature-controlling electronics, was located in the funnel attached to the inflow port (Figs. 1 and 2). The temperature controller, driving the heating elements located in the air hoses leading to each chamber, held the temperature to $\pm 0.2^\circ\text{C}$ for any temperature between about 26°C and 33°C.

Instrumentation

RF power was supplied by a CW generator (model 250C, Epsco) used with either a model M8045H (200-700 MHz) or a model M8060H (700-1200 MHz) plug-in oscillator, each capable of a maximum nominal power output of 250 W. For the 600- to 1200-MHz system, the RF generator was connected via RF 213/U coaxial cable through a dual directional coupler (either a model 3020A or model 3022, Narda) to a double-stub tuner (model 1778A, Maurey), which was in turn connected to the feedhorn of the anechoic chamber used for RFR exposure. The forward and reflected powers were measured by power meters (model HP 435A, Hewlett-Packard) with power sensors (model HP 8482H, Hewlett-Packard)

connected to the directional coupler ports. Direct measurements of RF field strength were made with a broadband isotropic radiation monitor (model 8606, Narda) fitted with a 0.3- to 26-GHz probe (model 8623, Narda).

Animal core temperatures were measured with two noninterfering temperature monitors (model 101, Vitek). Exhaust air temperature from each anechoic chamber was measured directly by a thermistor probe connected at the exhaust port of each enclosure. Two logging multimeters (model HP 3467A, Hewlett-Packard) were used to record power levels, exhaust air temperature, and, in some experiments, animal core temperatures. An airflow meter (model 1650, Thermo Systems) monitored the amount of air flowing through both the TEM chamber and the two anechoic chambers.

TECHNICAL APPROACH

Animals

Female strain CD-1 mice were purchased from Charles River Laboratories (Portage, MI) and housed in groups of 6 to 8 in polycarbonate cages covered with polyester filter bonnets. Their environment was controlled to maintain a 12/12-h light/dark cycle, an air temperature of 22^o-24^oC, and a humidity of about 40%. Purina Lab-Chow and water were provided ad libitum. The animals were 7-10 weeks of age when experiments were performed. Those included in each experiment were matched in weight, within $\pm 10\%$, and date of birth.

Chemicals

[¹⁴C]Thymidine ([¹⁴C]TdR; 53 mCi/mM) and [³H]deoxycytidine ([³H]CdR; 27 Ci/mM) were purchased from New England Nuclear. [³H]Thymidine ([³H]TdR; 15 Ci/mM) was from Schwarz/Mann. 5'-Bromodeoxyuridine (BrdUrd) and Hoescht dye 33258 were obtained from Calbiochem-Behring. Colcemid, cyclophosphamide, and hydroxyurea were products of Sigma. S₁ nuclease was purchased from Miles Laboratories, and Hae III restriction endonuclease was a product of Bethesda Research Laboratories. Sorensen's buffer tablets and R66 Giemsa stain were obtained from Bio-Medical Specialties. All other chemicals were reagent grade.

SAR and Power Density Measurements

SAR measurements were made at several frequencies between 600 and 1200 MHz, using mouse cadavers as test subjects. Both Dewar calorimetry and the noninterfering temperature probe technique (Durney et al., 1980) were used for the SAR measurements.

The vessels used for the calorimetric measurements were half-pint capacity Dewar flasks (model 215, Thermos) with a 3/4-in. layer of polyurethane foam molded around the vessels for added insulation. The thermal capacity of each Dewar was found to be 61 J/^oC when equilibrated with 35 ml of water. Test animals were killed by cervical dislocation, weighed, and

cooled to near room temperature by exposure to forced airflow. The cadavers were placed in insulated lossless containers (Styrofoam) and positioned in one of the RF chambers. After irradiation for 10 min with a known input power, the cadavers were immediately removed to the Dewars and allowed 1.5 h to reach thermal equilibrium with 35 ml of water. Frequent gentle agitation was used to augment the equilibration. The temperature of the cadaver at the moment of insertion in the Dewar was calculated using the formula described by Durney et al. (1980).

$$T_e = \frac{(Z_p + c_e m_e) T_F - T_I}{m_s c_s} + T_F \quad (1)$$

where:

- Z_p = thermal capacity of Dewar = 61 J/°C
- c_e = specific heat of water = 4185 J/°C per kg
- m_e = mass of water in Dewar = 0.035 kg
- T_F = final temperature of water, Dewar, and mouse
- T_I = initial temperature of water and Dewar
- m_s = mass of the mouse (0.025 to 0.030 kg)
- c_s = specific heat of mouse = 3448 J/°C per kg

The SAR for the mouse is given by:

$$\text{SAR} = \frac{c_s (T_e(\text{exposed}) - T_e(\text{sham}))}{\text{exposed time in seconds}} \text{ W/kg} \quad (2)$$

Temperature changes in RF-irradiated test subjects were measured by a noninterfering technique using the Vitek 101 probe. SAR was calculated by multiplying the per second increase in temperature of each irradiated subject by its specific heat (for mice, 3448 J/°C per kg). Thus,

$$\text{SAR} = 3448 \left(\frac{\Delta T}{\Delta t} \right) \text{ W/kg} \quad (3)$$

where ΔT is the temperature rise in °C and Δt is the duration of irradiation in seconds. The rate of temperature increase was measured by two methods and compared. In one case the initial core temperature was subtracted from the maximum core temperature (reached a short time after the RF power was turned off), and then divided by the duration of irradiation. A slightly different approach was to measure the slope of the temperature rise after steady-state temperature rise appeared to be reached. These two methods gave essentially the same result.

For normalized SAR, the calculated SAR values were divided by the power density incident on the subject. The power density is given by:

$$P_d = \frac{0.65 A P_t}{\lambda^2 d^2} \text{ W/m}^2 \quad (4)$$

where A is the horn aperture in m^2 , P_t is the power in watts radiated from the horn, λ is the wavelength in meters, and d is the distance from the center of the subject to the horn aperture. The radiated power, P_t , is found from measurements of forward and reflected power as recorded by power meters PM1 and PM2 respectively. Referring to Figure 3,

$$P_t = (PM1)10^{(K_f-L)/10} - (PM2)10^{(K_r+L)/10} \quad (5)$$

where K_f and K_r are the coupling factors of the directional coupler ports expressed in dB, and L is the cable loss between the directional coupler and feedhorn, also expressed in dB. Power meter PM1 monitors forward power; and PM2, reflected power.

Core Temperature Measurements

Colonic-temperature measurements were made in unanesthetized mice (25-29 g). Each animal was secured in a Plexiglas restraining cage, and the tip of a Vitek probe was inserted 1 cm into the rectum. The probe was held in place by taping it to the support bar of the Plexiglas cage. Colonic temperatures were recorded at 1-min intervals for 2-3 h with the animals maintained under various conditions. These included baseline recordings (no RF power) during exposure to nonflowing ambient air and recordings during exposure to forced airflow both in the absence and presence of RFR. Colonic temperature responses to variation of air temperature were also monitored.

Intravenous Infusion

Solutions of BrdUrd and radioactive thymidine were given intravenously (iv) to the test animals. The specially constructed Plexiglas cages used to restrain the animals are described elsewhere (Brown et al., 1981). Some experiments in this study involved iv infusion concomitant with RFR exposure, requiring substitution of nonmetallic materials for conventional needles to avoid perturbations of the E-field. This requirement was satisfied by using Teflon cannulae. A sharpened 28-gauge stainless-steel wire was inserted in a lateral tail vein and used to guide a 3-cm cannula, prepared from 0.038-cm (i.d.) Teflon tubing, into the vessel as described by Brown et al. After completing the cannula insertion, the steel guide was removed and the exposed end of the cannula was connected to a 150-cm length of Teflon tubing attached to a saline-filled 1-cc syringe. A syringe pump (model A-D, Razel) was used to introduce infusion solutions into the animals at a flow rate of 0.2 ml/h. The Teflon cannula permitted routine, continuous iv infusions for about 26 h.

Other *in vivo* experiments involved *iv* infusions for 2-3 h immediately prior to RFR exposure. For these short-term infusions, a 26-gauge stainless-steel needle attached to a 150-cm length of tubing was inserted in a lateral tail vein of a restrained animal. Saline was infused at 0.2 ml/h.

DNA Synthesis Measurement

The protocol used to monitor DNA synthesis in intact mice, adapted from a procedure described by Brown et al. (1970), involved dual isotope labeling. Basically, the effect of irradiation was assessed by comparing incorporation of an ^3H -labeled DNA precursor during RF (or sham) irradiation with the level of ^{14}C labeling of DNA before commencing irradiation.

Mice were placed in the restrainers, cannulated as described for short-term infusion, and *iv* administration of 0.15 M NaCl was initiated. Each animal received a single bolus injection of [^{14}C]TdR (0.2 ml; 2.5 $\mu\text{Ci/ml}$) delivered via the cannulation tubing. After 90 min, [^3H]TdR (0.2 ml; 50 $\mu\text{Ci/ml}$) was given, the cannula quickly removed, and the animal immediately transferred to either an RFR-exposure chamber or a sham-exposure chamber. The time from [^3H]TdR injection to placement in the exposure chamber was about 40 s. Positive control animals received hydroxyurea (0.1 ml) 5 min before the [^3H]TdR. Each animal was removed from the chamber and killed by cervical dislocation 20 min after the injection of [^3H]TdR. The spleen and both femurs were quickly removed to liquid N_2 . Time from sacrifice to freezing was about 30 s for the spleen and 90 s for the femurs. The protocol for injecting radioactive precursors to pulse label DNA *in vivo* is presented in Figure 4.

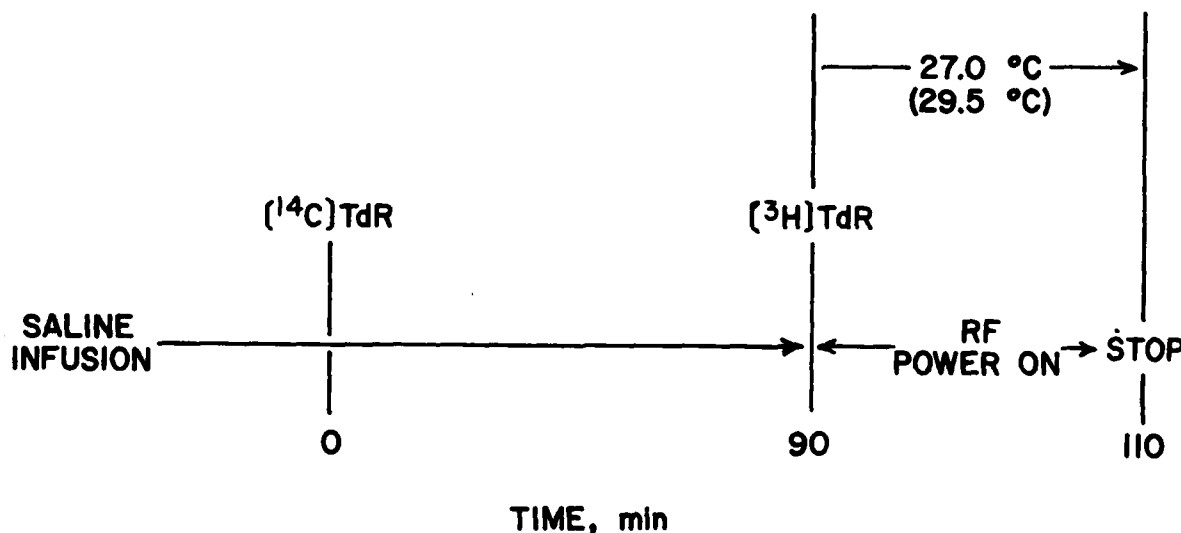


Figure 4. Protocol for injecting radioactive precursors to label DNA in the spleen and marrow tissue of mice. The temperature indicated is for air ventilating the anechoic chambers during 800- or 1200-MHz exposures; the value in parentheses, air temperature in the TEM chamber during 400-MHz exposures. Sham anechoic chambers were maintained at 29.5°C; the sham TEM chamber, at 30.5°C.

Spleen specimens were thawed and homogenized in 9 volumes of 0.1 M citric acid with a Dounce homogenizer. The homogenate was passed through a 110-mesh nylon screen, and the filtrate was centrifuged for 10 min at 900 g. The pellet was resuspended in citric acid and carefully layered over an equal volume of 0.34 M sucrose-0.18 mM CaCl_2 . The pellet collected by centrifugation at 900 g was dissolved in 1 ml of 0.1 M NaOH and incubated for 30 min at 60°C. After cooling, 10 ml of ice-cold 10% trichloroacetic acid was added and the acid insoluble radioactivity collected on Whatman GF/B glass-fiber filters. The filters were washed with ethyl alcohol, dried, and immersed in 5 ml of a toluene-PP0 solution. Radioactivities were assayed in a liquid scintillation counter (model LS 7500, Beckman) and converted to disintegrations per min (DPM) by correcting for ^{14}C overlap into the ^3H channel (about 9%) and sample efficiencies (about 30% for ^3H and 62% for ^{14}C). Results were expressed as ^3H DPM/ ^{14}C DPM ratios.

Femurs were thawed and flushed with isotonic saline to remove marrow tissue. The pellet of marrow cells collected by centrifugation for 10 min at 900 g was dissolved in NaOH and heated at 60°C as described for the spleen samples. Acid insoluble radioactivity was measured, and results were expressed as ^3H DPM/ ^{14}C DPM ratios.

Sister Chromatid Exchange Analysis in Vivo

The procedure used to visualize SCE involved BrdUrd labeling of replicating DNA followed by differential staining of metaphase chromosomes. Fresh solutions of BrdUrd, 6.5 mg/ml 0.15 M NaCl, were infused in restrained animals at a dosage of 50 $\mu\text{g}/(\text{g}\cdot\text{h})$ for 24 h, a period sufficient to permit completion of two division cycles (Schneider et al., 1978). RFR- and sham-exposures, 8-h total duration, were initiated 1 h after beginning the BrdUrd infusion. Colcemid, 0.4 $\mu\text{g}/\text{g}$, was given iv 2 h before conclusion of the BrdUrd infusion to arrest dividing cells in metaphase. The protocol for BrdUrd labeling and air temperature adjustments is shown in Figure 5.

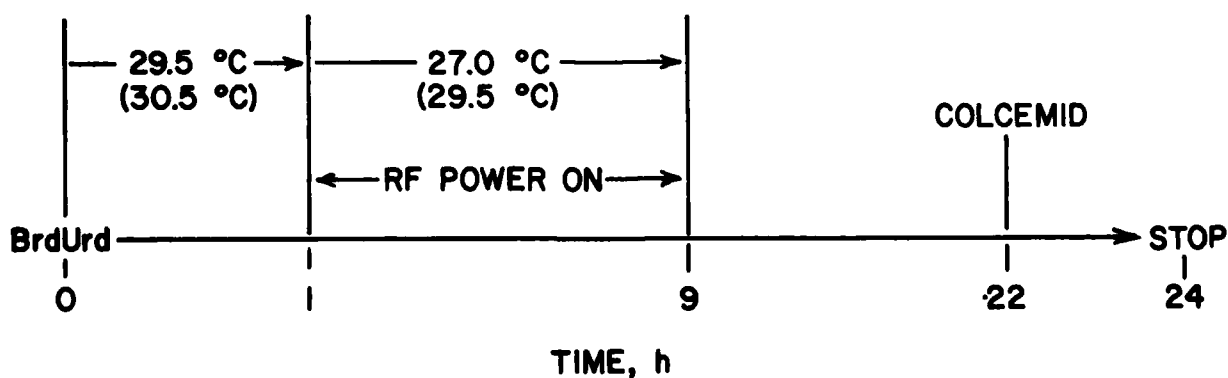


Figure 5. Protocol for administering BrdUrd and colcemid to mice for SCE analysis in marrow tissue. Temperatures indicated are for air ventilating the anechoic chambers used for the 800- and 1200-MHz experiments; values in parentheses, air temperatures in the TEM chamber for the 400-MHz experiments. Sham-irradiation enclosures were maintained at temperature levels used during the first hour of the BrdUrd infusion. Forced airflow was terminated at the conclusion of the RFR exposure.

Animals were killed by iv injection of air. Femurs were quickly removed from each animal, and marrow cells were collected by forcing hypotonic KCl (0.06 M) through the marrow channels. After a 30-min incubation at 37°C, the swollen cells were pelleted by a 400-g centrifugation and resuspended in fixative, 3:1 methanol-acetic acid. Resuspension in fixative was repeated twice. Metaphase spreads were prepared by placing drops of the cell suspension on cold wet slides as described by Lubs et al. (1973).

Differential staining of sister chromatids was by the fluorescence-plus-Giemsa method of Perry and Wolff (1974) as modified by Minkler et al. (1978). After aging for at least 4 days, slides were stained for 30 min in 10 µg/ml Hoescht 33258 in Sorensen's buffer, pH 6.8. The slides were rinsed in DH₂O, mounted in Sorensen's buffer, and placed under a UV-light source (model M-218, Colight) equipped with a 400-W mercury lamp. Ultraviolet exposure was for 45 min at a distance of 46 cm. Coverslips were then removed and the slides were incubated 1 h at 52°C in 0.3 M NaCl-0.01 M Tris, pH 10. Slides were rinsed in DH₂O and stained for 5-10 min in 5% Giemsa in Sorensen's buffer. Air-dried slides were cleared with xylene and coverslips were mounted.

Slides were viewed under a Zeiss standard microscope fitted with a 35-mm photomicrography system (model PM-10, Olympus). Differentially stained chromosomes of second-division-cycle cells (at least 15 for each animal) were photographed on Kodak Tech-Pan film. Prints of each metaphase spread were prepared, coded, and examined blind for SCE scoring.

S₁ Nuclease Assay

As substrates for the nuclease assay we chose ³H-DNA isolated from CHO-K₁ cells labeled with [³H]TdR or [³H]CdR. DNA was isolated by proteinase K digestion of cellular lysates, using a modification of the procedure of Gross-Bellard et al. (1973). Briefly, cells were lysed and digested by a 16-h incubation in buffer A containing 0.15 M NaCl with 200 µg/ml proteinase K (Beckman). Crude DNA was removed from the lysate by adding two volumes of cold ethyl alcohol followed by gentle spooling on a glass rod. The DNA was redissolved in buffer A. Proteinase K was added and the 16-h digestion repeated. After cold ethyl alcohol was added, DNA was again collected on a glass rod and then redissolved in 0.15 M NaCl. The S₁ nuclease reactions, essentially as described by Ando (1966) and Vogt (1973), consisted of 0.3 M NaCl, 0.1 mM ZnSO₄, 5% glycerol, and 25 mM sodium acetate, pH 4.5, plus enzyme and substrate as indicated. Preliminary tests of enzyme and substrate were performed with 0.5-ml volumes. For tests of RFR effects, 0.14-ml volumes of the reaction mixture were loaded into glass capillary tubes, 4 cm x 1.3 mm (i.d.). The ends of the tubes were sealed with small glass beads held in place with silicone tubing, and the tubes were then placed either in an RFR enclosure parallel to the E-field with air temperature maintained at 37.4°C or in a 37.4°C water bath. Incubations were for 30 or 60 min. Reactions were halted by placing the tubes in an ice slurry, then adding 1.0 ml of 7% TCA to the reaction mixture. The acidified reaction mixture was passed through either a Millipore filter or a Whatman GF/B glass-fiber filter to separate the acid-soluble and acid-insoluble radioactivities. Aliquots of the filtrate were counted in Aquasol (New England Nuclear) liquid scintillation solution to assess the release of radioactive 5'-mononucleotides by the nuclease.

RESULTS AND DISCUSSION

Power Density and Field Uniformity

Measurements were made of absolute power levels along the work deck within each of the two anechoic chambers. The center of the RF probe was 5.1 cm above the deck, or about 2.5 cm higher than the center of a cage-restrained mouse. Power density values obtained by direct measurement were compared with power density values calculated by equation 4. Ratio comparisons of these values are presented in Figure 6. The measured and calculated values for the large-horn chamber were essentially in agreement. For the small-horn chamber these values obtained at 1200 MHz were also in agreement; but at 900 MHz, the power-density value measured for the small-horn chamber was 65% higher than the corresponding calculated value. Furthermore, the SAR values obtained for subjects exposed to RFR in the small-horn chamber were higher than the SAR values reported by Durney et al. (1978) for large-mouse models exposed at 900, 1000, and 1100 MHz. The feedhorns are scaled such that the wave pattern emitted from the large horn at 800 MHz should be the same as that from the small horn at 1200 MHz, the 700-MHz pattern for the large horn the same as that for the small horn at 1050 MHz, etc. We are unable to offer an explanation for the discrepancies with the small horn. Because the anechoic material functions as a more effective absorber at higher frequencies, we might have expected better agreement between the measured and calculated power density values at higher rather than lower frequencies.

The uniformity of the power-density pattern was measured at 800 MHz in the large-horn chamber and at 1200 MHz in the small-horn chamber. The results obtained are plotted in Figures 7 and 8. Uniformity was essentially as expected from an open-ended waveguide in the TE_{10} mode. The absence of any significant cyclic variation of power density as a function of position on the deck indicates that no significant standing waves were present.

SAR Measurements

SAR measurements obtained by Dewar calorimetry and the noninterfering temperature-probe technique for subjects exposed to RFR in the anechoic chambers are summarized in Figure 9. The values shown represent normalized SAR, that is, SAR expressed in relation to the calculated power density. Power density was calculated, using equations 4 and 5, from power-meter readings of forward and reflected power. The solid curve in Figure 9 represents average SAR values for prolate spheroid models of large mice and was redrawn from a similar curve in Figure 38 of the Dosimetry Handbook, 2d ed. (Durney et al., 1978). Also included, for comparison, is a dashed line representing SAR measurements obtained previously for subjects exposed to 200- to 400-MHz fields in the TEM chamber (Brown et al., 1981). The dashed line has a slope of 0.7 on the log-log graph and intersects the Dosimetry Handbook curve at about 900 MHz.

Two points on the graph of SAR data are particularly noteworthy--the 800- and the 1200-MHz values. The SAR values we obtained at 1200 MHz by

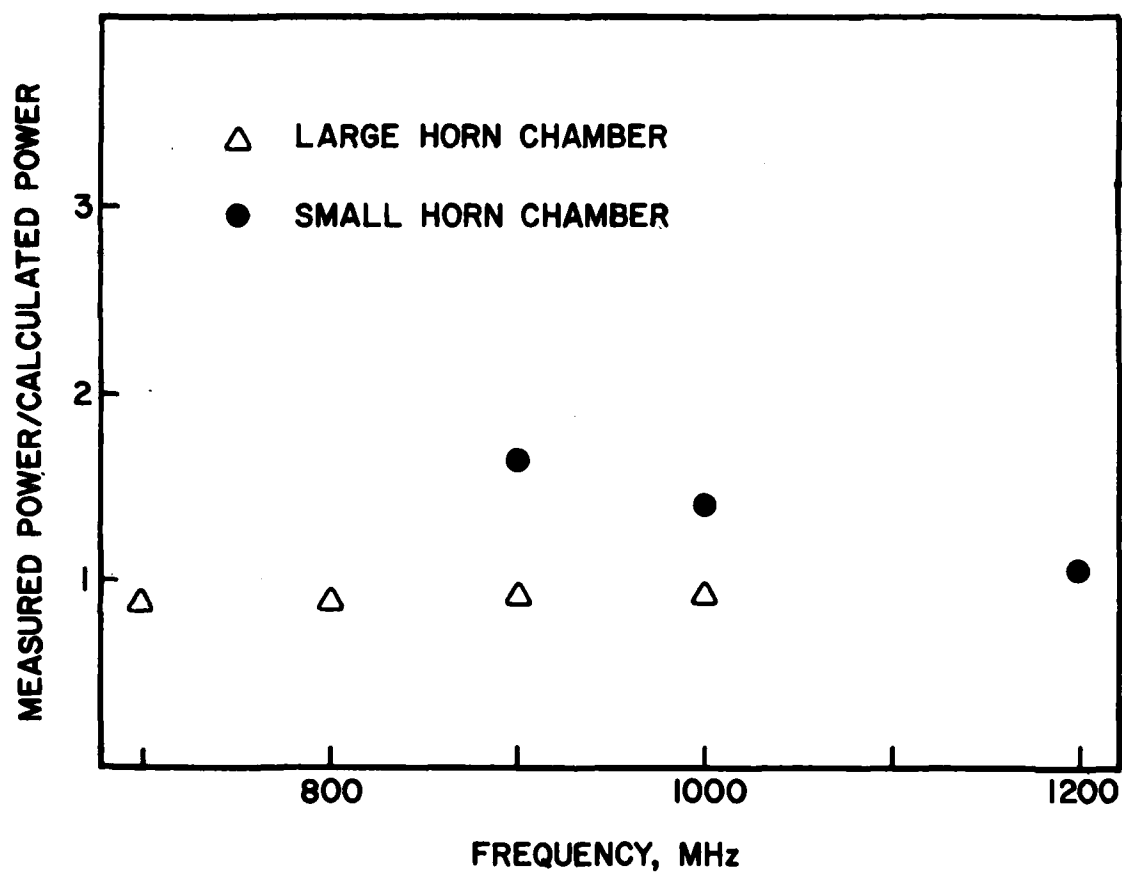


Figure 6. Ratios of measured power-density values to calculated power-density values for the anechoic chambers. Direct measurements of power densities were made with a broadband radiation monitor. Meter readings of forward and reflected power were used to calculate power density by equation 4.

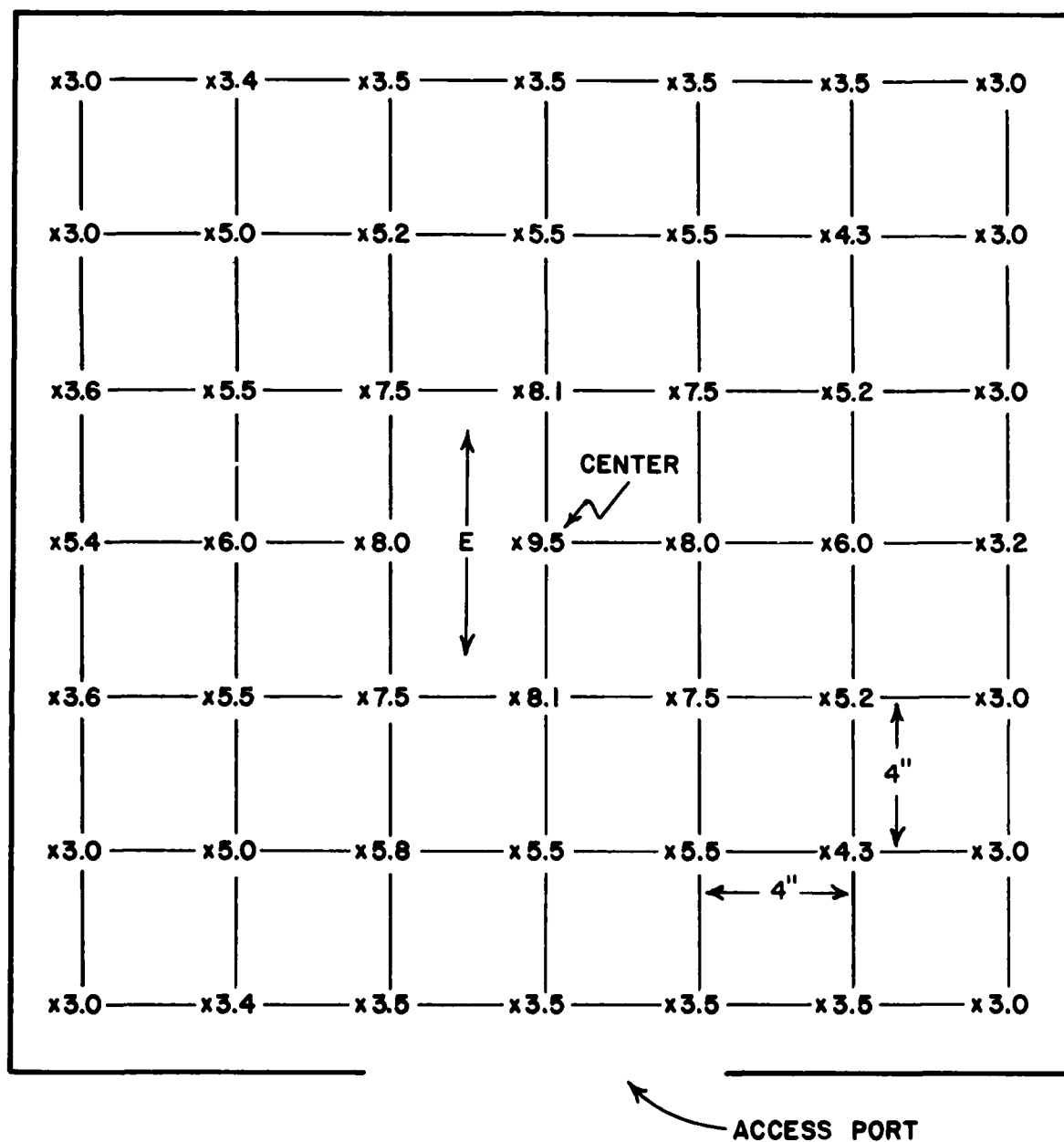


Figure 7. Power densities along the work surface of the large-horn anechoic chamber. Measurements were made at 800 MHz, and values are expressed in mW/cm^2 .

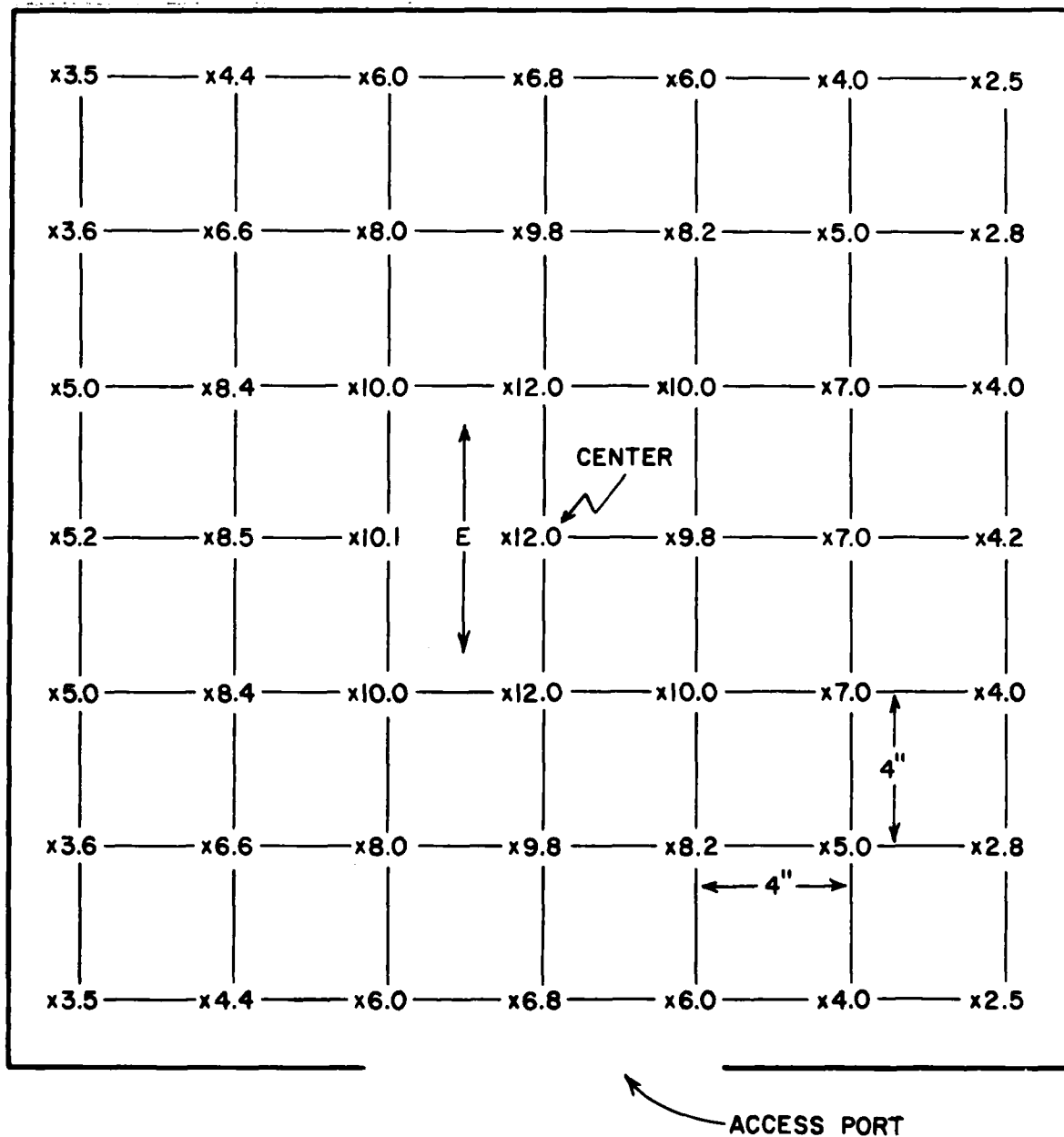


Figure 8. Power densities along the work surface of the small-horn anechoic chamber. Measurements were made at 1200 MHz, and values are expressed in mW/cm^2 .

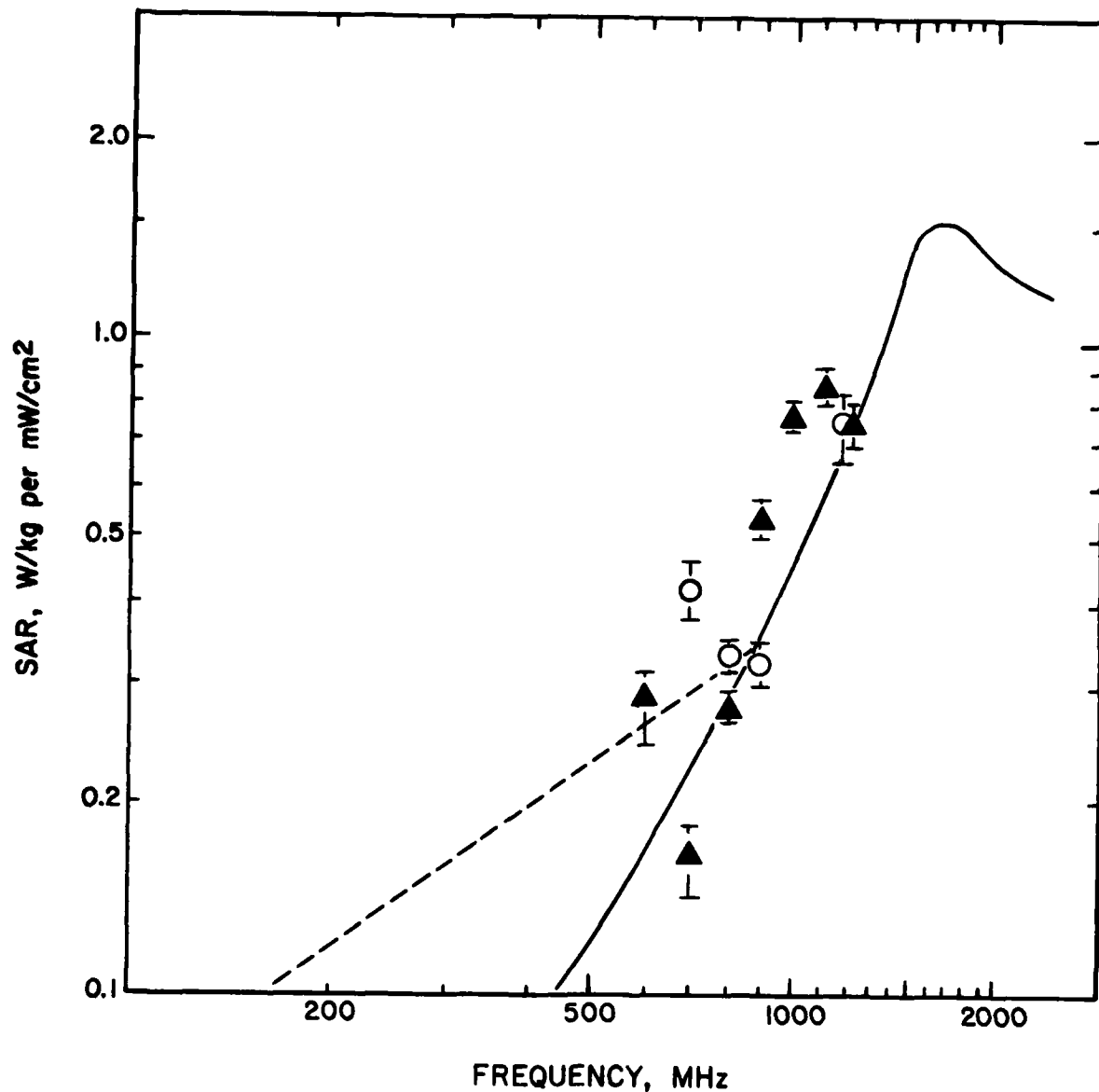


Figure 9. SAR values measured for mouse cadavers exposed to 600-1200 MHz. Measurements were performed by Dewar calorimetry (O) or the non-interfering temperature-probe technique (▲). Each point represents the mean of six determinations, one cadaver per trial; and vertical brackets are standard error of the mean. The solid curve was redrawn from the Dosimetry Handbook, 2d ed. (Durney et al., 1978) and represents SAR values for prolate spheroid models of the large mouse. Also included for comparison is a dashed line representing a best fit to SAR values obtained for mouse cadavers exposed to 200-400 MHz (Brown et al., 1981).

both measuring methods are essentially identical and agree with the 1200-MHz point on the solid curve redrawn from the Dosimetry Handbook. And at 800-MHz, SAR values by both our methods are similar and again match the SAR value for the spheroid models. The disparity between our SAR means at 900 MHz may be attributed to the use of different anechoic chambers. The calorimetric measurements of SAR at 900 MHz were performed with subjects irradiated in the large-horn chamber, and the small-horn chamber was used for SAR measurement by the noninterfering temperature-probe method. As noted in the preceding section of this report, for the small-horn chamber the power density measured at 900 MHz differed appreciably from the corresponding calculated value. If the actual power density at 900 MHz in the small-horn chamber was higher than the calculated power density, as suggested by the measurements discussed in the preceding section, then the mean for the SAR values obtained by the noninterfering temperature-probe method should lie closer to the spheroid-model SAR value represented by the 900-MHz point on the solid curve (Fig. 9). Disparity between calorimetric and noninterfering-temperature-probe SAR data was particularly striking at 700 MHz. The disparity at that frequency was not the result of using different chambers--both sets of measurements were performed using the large-horn chamber. The reason for this dissimilarity is not clear.

A major objective of this investigation was exposure of animal subjects to RF power densities equivalent to an absorbed dose of 4 W/kg at each of the three test frequencies: 400, 800, and 1200 MHz. Early in the investigation numerous measurements of incident power densities and SAR were performed and the values were correlated in an effort to determine the adjustments needed for the desired absorption level. As shown in Figure 9, the experimental SAR data for mouse cadavers irradiated in the 600- to 900-MHz frequency range falls on a straight line extrapolated from our earlier 200- to 400-MHz SAR data for subjects irradiated in the TEM chamber. And, a log-log plot of our SAR data for cadavers irradiated in the 900- to 1200-MHz range appears to nearly fit a straight line connecting the 900- and 1200-MHz points on the curve redrawn from the Dosimetry Handbook. Thus, the curve fitting our experimental SAR data appears to be biphasic, with a slope of 0.7 over the 200- to 900-MHz range and a slope of 2.6 over the 900- to 1200-MHz range. Using the experimental curve described, we estimated that exposures of E-oriented mice to incident power densities of 12.5 and 5.3 mW/cm² would result in an absorption level of 4 W/kg at 800 and 1200 MHz respectively. Accordingly, these incident-power densities were used in subsequent experiments conducted at these two frequencies.

SAR measurements can be used to indirectly determine power density. For an SAR level of 4 W/kg, for example, the power density required may be determined by the expression

$$P_{dreq'd} = \frac{4}{(SAR)_{norm}}$$

The power meter settings needed to reach the above power density may be determined from equation 5. Two adjustments are required before the power setting can be finalized. First, a position correction is required when two mice are in the chamber. Neither mouse is positioned directly beneath the center of the horn. A 5% decrease in power density may be estimated for

this off-center position, based on consideration of the theoretical pattern of waves radiated from an open-ended waveguide plus consideration of the maps of the measured power densities (Figs. 7 and 8). The second adjustment is concerned with our observation that the Plexiglas restraining cages enhance SAR by a factor of 1.34, as revealed by our earlier measurements performed in the TEM chamber (Brown et al., 1981). The SAR data represented in Figure 9 were obtained with mouse cadavers not placed in Plexiglas restrainers during RF irradiation.

The following example will illustrate how the required power-meter setting may be obtained for 4-W/kg SAR at 800 MHz. The normalized SAR for mice exposed to that frequency may be estimated from Figure 9 to be 0.32 W/kg per mW/cm². The power density needed for an SAR of 4 W/kg should be, therefore, 4/0.32 mW/cm², or 12.5 mW/cm². Equations 4 and 5 are then used to determine the power meter settings required for the desired power density. With PM1 reading 1 W and the double-stub tuner adjusted such that PM2 reads approximately zero, the 800-MHz power density along the chamber work surface is calculated to be 9.92 mW/cm². Since the power density desired in this example is 12.5 mW/cm², the PM1 power meter reading should be 12.5/9.92 W, or 1.26 W. When further corrected for both the position effect and the cage effect, the final setting needed for the desired power becomes

$$PM1 = (12.5/9.92)(1.05)(\frac{1}{1.34}) = 0.99 \text{ W}$$

Similar calculations are required for each frequency tested.

Airflow through TEM and Anechoic Chambers

Air flowing through the TEM chamber, and its corresponding sham enclosure, was measured at the center test position on either side of the center conductor. The velocity of airflow through these two chambers fluctuated over a range of 80-90 ft per min. Inflow air was directed to the work surfaces of the anechoic chambers via cardboard channels. Two longitudinal vanes in the cardboard channel were used to partition the airflow. Other vanes, placed in the Plexiglas funnel leading to the channel, were used to tune the airflow so that the air discharged along the 25-cm orifice of the channel was as uniform as possible. Flow across the work surface of each anechoic chamber fluctuated between 100 and 120 ft per min.

Core Temperature: RFR Subjects

This investigation was designed to test the inference of Prohovsky and colleagues that RFR interaction with duplex DNA may result in frequency-specific denaturation at exposed ends of the polymer. An important criterion for the in vivo phases of the investigation was avoidance of RFR-induced hyperthermia, to try to preclude heating artifacts. Indeed, hyperthermia has been observed to increase the frequency of SCE in cultured cells (Livingston and Dethlefsen, 1979).

Numerous baseline measurements of colonic temperature were conducted in our lab over the past 2 years. Restrained subjects used for these measurements were positioned either on the open lab bench or in one of the RFR enclosures. Colonic temperatures recorded at 60-s intervals for 2-3 h were graphed for analysis. Approximately 1 h was required before the initially agitated animals displayed what appeared to be a stable baseline temperature. These measurements, performed with the airflow turned off, revealed a mean colonic temperature of about 37.4°C. Subjects positioned in the TEM chamber with RF power off were found, as part of a prior project, to maintain their colonic temperature at this baseline level with the air blower activated and the air temperature adjusted to 30.5°C.

Mean colonic temperatures of mice subjected to different levels of 400-MHz power in the TEM chamber with a constant 30.5°C airflow are presented in Figure 10. The figure, taken from the 1981 report by Brown et al. shows that the test animals underwent a linear increase in body temperature as a function of the incident power density, with an apparent threshold of about 12 mW/cm² under the conditions used. We further observed that adjustment of the airflow temperature would compensate for RFR-induced hyperthermia, thereby permitting the colonic temperature of irradiated subjects to return to essentially baseline levels. Figure 11 shows the colonic temperature of subjects exposed to 400 MHz at power densities of 16 or 80 mW/cm² with an air temperature of 30.5°C. Reducing the air temperature from 30.5°C to 29.5°C appeared to compensate for the core heating elicited by the lower power density, and a reduction to 22.5°C seemed to compensate for the higher power level.

Thermal responses of mice irradiated at 800 and 1200 MHz in the anechoic chambers were also tested. Initial tests were performed with the airflow activated and RF power off. The results of several preliminary tests revealed that the animals held their colonic temperatures closest to the baseline when the temperature of the airflow through the anechoic chamber was adjusted to 29.5°C. With the airflow maintained at that temperature, we tested the thermal response of the animals to 800 and 1200 MHz at incident power densities calculated to be equivalent to SAR levels of 4, 6, or 8 W/kg (Fig. 12). The power densities required for the 800-MHz exposures were calculated to be 12.5, 18.8, and 25 mW/cm² respectively; for the 1200-MHz exposures, 5.3, 7.9, and 10.6 mW/cm² respectively. Figure 12 shows that exposure to 800 or 1200 MHz at power densities equivalent to 4 W/kg caused the body temperature to increase approximately 0.5-0.6°C; at 8 W/kg, more than 1.5°C.

Colonic temperatures of animals positioned in the anechoic chambers and exposed to forced airflow maintained at different temperatures are shown in Figure 13. For animals subjected to forced airflow adjusted to 29.5°C, the mean colonic temperature was essentially the same as the baseline level. (The baseline temperature of mice exposed to non-flowing ambient air appeared to be about 37.4°C.) Figure 13 also shows that adjusting the ventilating air temperature down to 27.0°C resulted in approximately a 0.5°C drop in the colonic temperature of the mice. Based on the findings represented in Figures 12 and 13, we concluded that during exposure to 800- or 1200-MHz at incident power densities equivalent to an SAR of 4 W/kg, adjusting the air temperature to 27.0°C would compensate for the RF heating and allow the irradiated animals to maintain their core temperatures at essentially the baseline level.

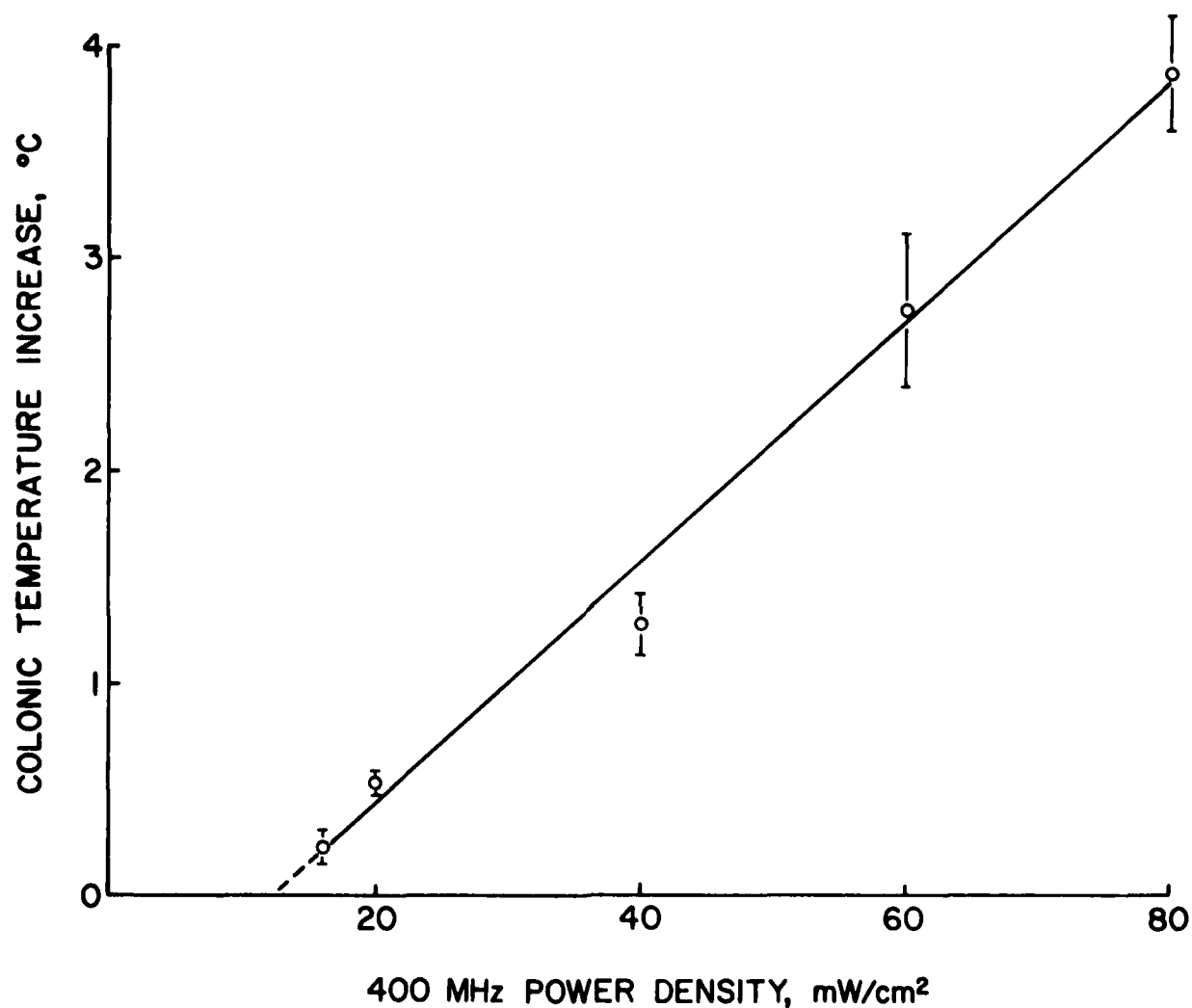


Figure 10. Change in colonic temperature of mice exposed to 400 MHz. Subjects were positioned in a TEM chamber ventilated with 30.5°C airflow. Each point is mean of eight determinations, and vertical bars are standard error of the mean. (Figure from Brown et al., 1981).

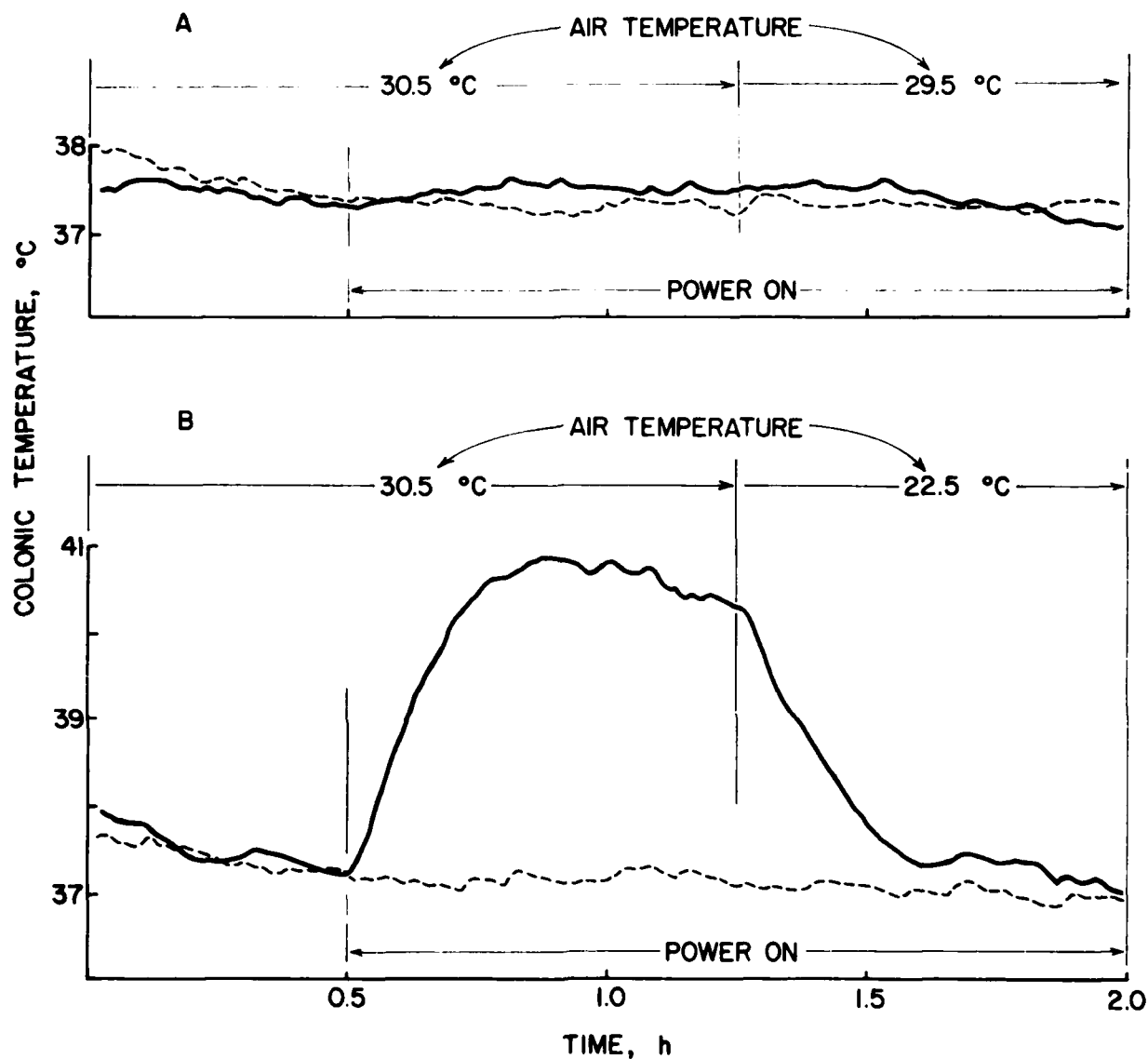


Figure 11. Colonic temperature of irradiated mice adjusted by air-temperature variation. Solid tracings represent the colonic temperatures of mice exposed to 400-MHz power densities of (A) 16 mW/cm² or (B) 80 mW/cm². Air temperature was adjusted as indicated 45 min after commencing RF irradiation. Dashed tracings represent the baseline temperatures of the same animals exposed for 2 h to ventilating air maintained at 30.5°C (no RFR).

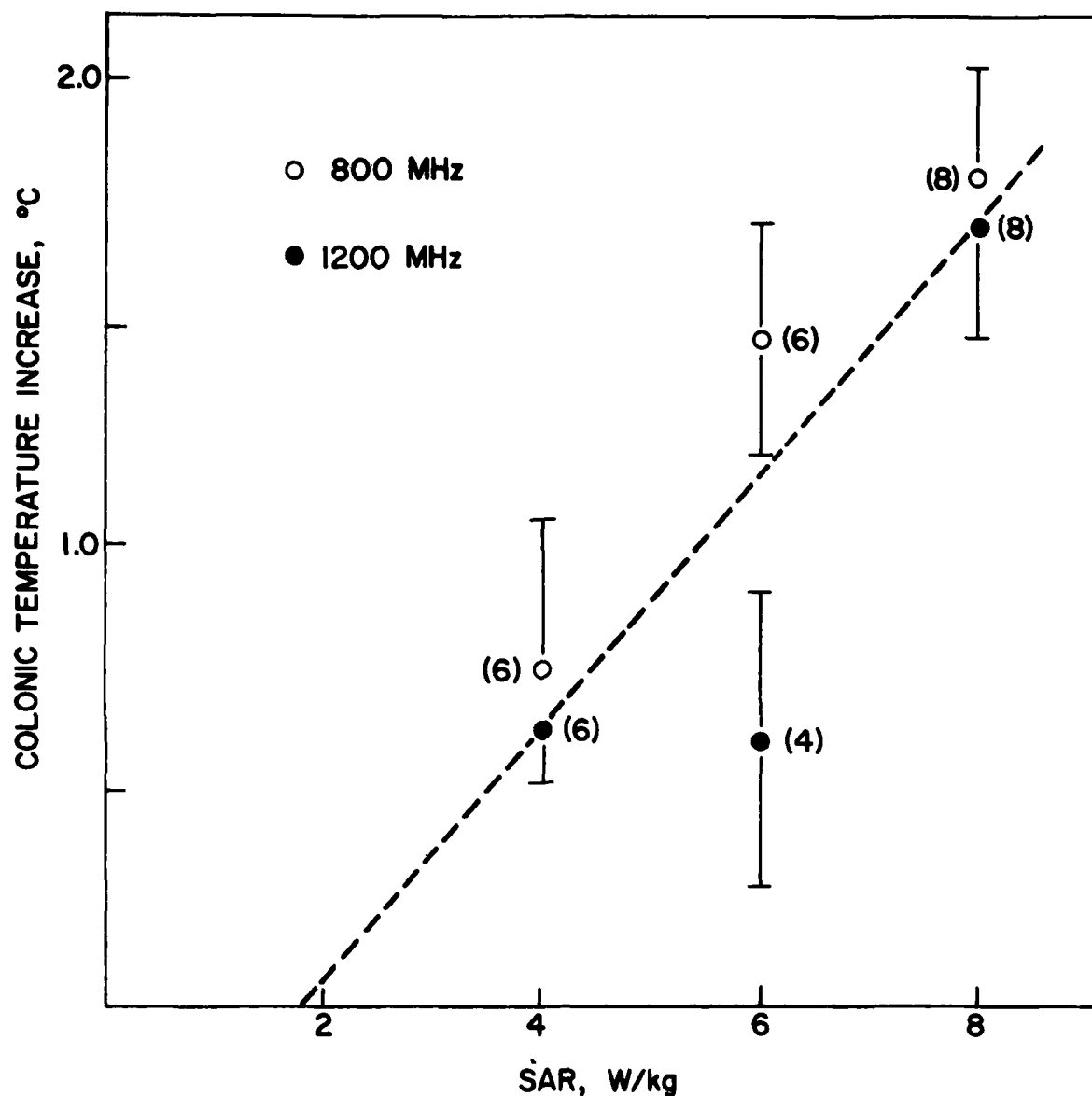


Figure 12. Change in colonic temperature of mice exposed to 800 and 1200 MHz. Animals were positioned in an anechoic chamber maintained at 29.5°C and subjected to incident RF power densities equivalent to the absorbed doses indicated. Each point is a mean of the number of observations in parentheses. Vertical brackets are standard error of the mean. The dashed line represents a least-squares fit to the data points. (The baseline temperature of nonirradiated control subjects was about 37.4°C.)

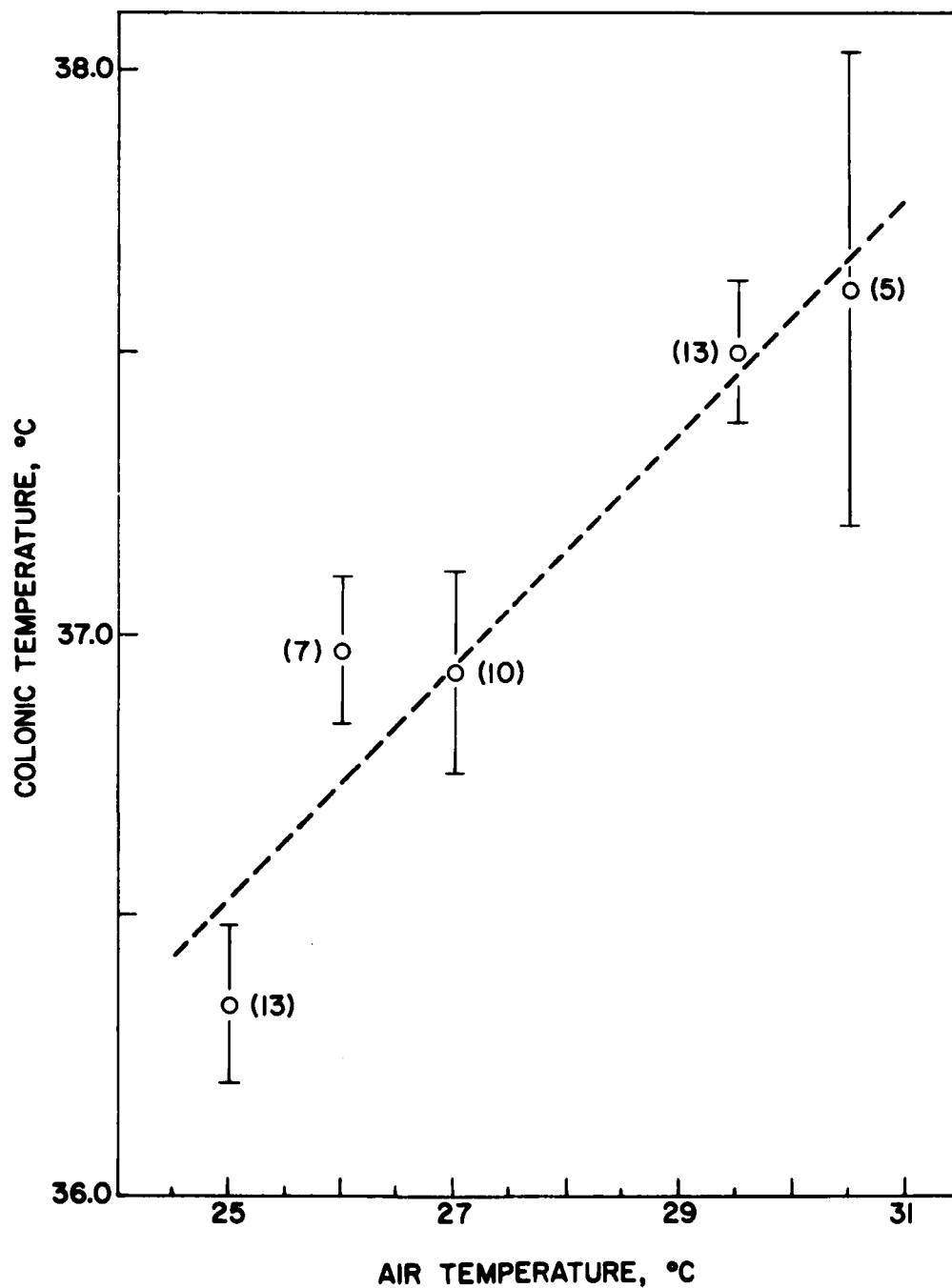


Figure 13. Colonic temperatures of mice exposed to different temperatures of forced airflow ventilating the anechoic chambers. Each point is a mean of the number of observations in parentheses. Vertical brackets are standard error of the mean. The dashed line represents a least-squares fit to the data points.

Sister Chromatid Exchange: RFR Effects

Analysis of SCE has proven to be a sensitive cytogenetic method of detecting mutagenic/carcinogenic agents both in vitro (Carrano et al., 1978; Perry and Evans, 1975) and in vivo (Schreck et al., 1979). Although the nature of SCE is unclear, it may be linked with DNA postreplication repair (Schneider et al., 1978), a mechanism thought to involve recombination (Lehmann, 1974). Our rationale for including SCE analysis in this project was that an increase in recombination events, manifested as an elevated SCE frequency, could occur if absorption of RF photons by DNA induces partial denaturation of the macromolecule as suggested by Prohofskey and colleagues (Putnam et al., 1981).

The method of SCE analysis used in this investigation, adapted from Perry and Wolff (1974), involved BrdUrd labeling of replicating cells for a duration roughly twice that of the cell cycle, followed by fluorescent-plus-Giemsa differential staining of the chromosomes. After two replication cycles in the presence of BrdUrd, the chromatids containing BrdUrd in both strands of DNA stain weakly with Giemsa while the chromatids containing DNA in only one strand stain darkly with Giemsa.

Bone marrow cells were chosen for analysis in this investigation. Figure 14 shows fluorescent-plus-Giemsa-stained metaphase chromosomes of marrow cells after one, two, or three replications in the presence of BrdUrd. As shown, first-division-cycle cells yield chromosomes that stain darkly. In second-division-cycle cells, each metaphase chromosome consists of one light and one dark chromatid. In each third-division-cycle cell, half of the chromosomes consist of two light chromatids while the remaining chromosomes each consist of one light and one dark chromatid. Only second-division-cycle cells were used to score SCE frequencies in this study.

Mice treated with cyclophosphamide, a known SCE-inducing agent (Schreck et al., 1979), were included in some experiments as positive controls to test the effectiveness of the assay in our hands. All animals subjected to the cyclophosphamide treatment exhibited increased SCE frequencies. Examples of metaphase chromosomes from animals treated with cyclophosphamide at concentrations of 0, 10, or 20 mg/kg are shown in Figure 15. Individual SCE values observed in two cyclophosphamide titration experiments are listed in Table 1. Both the figure and the table show that the SCE frequency increased as a function of cyclophosphamide concentration. Treatment of mice with cyclophosphamide at a dosage of 10 mg/kg has been reported both by Schneider et al. (1981) and Schreck et al. (1979) to induce about 24 SCE per marrow cell. The SCE frequencies we observed at this dosage were, as shown in Table 1, about 19 per cell in the first experiment and about 26 per cell in the second. The similarity of our results to reported values attests to the overall reliability of the assay in our hands.

Examples of differentially stained metaphase chromosomes from mice that were sham-irradiated or exposed to either 400-, 800-, or 1200-MHz radiation are presented in Figure 16. Mean numbers of SCE observed in the bone marrow cells for each animal in the eight experiments completed for this portion of the investigation are presented in Table 2. An overview of these data does not reveal any overt differences between the SCE values of control and

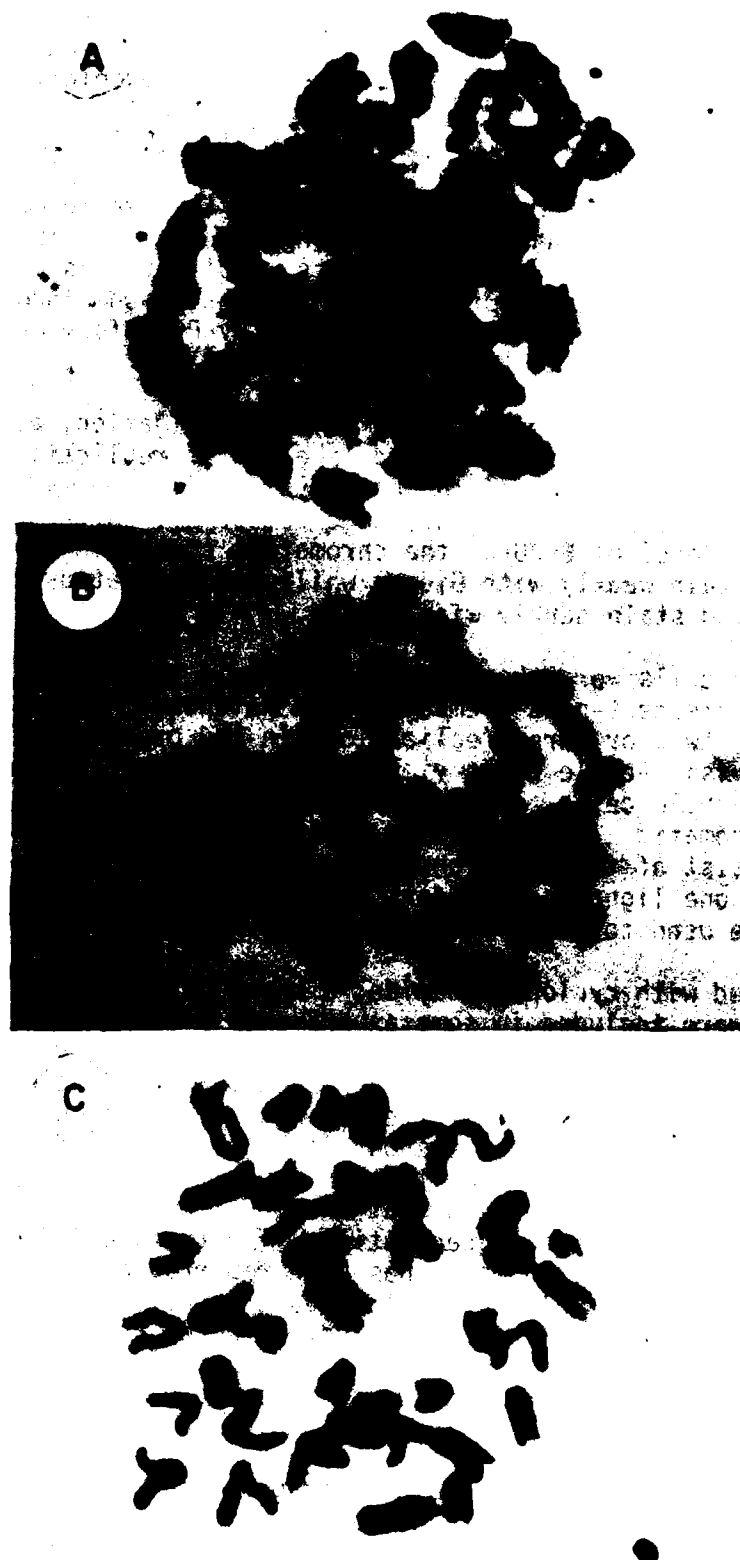


Figure 14. Appearance of fluorescent-plus-Giemsa-stained metaphase chromosomes from the bone marrow of mice.
 A. First-division cycle cell; B. Second-division-cycle cell; C. Third-division-cycle cell.



Figure 15. Differentially stained second-division-cycle marrow chromosomes from mice treated with different concentrations of cyclophosphamide. A. 0 mg/kg; B. 10 mg/kg; C. 20 mg/kg.

TABLE 1. CYCLOPHOSPHAMIDE INDUCTION OF SCE IN BONE MARROW OF MICE

Experiment	Cyclophosphamide (mg/kg)	No. cells scored/animal	SCE/cell (Mean \pm S.E.M.)
1	0	11	3.6 \pm 0.9
		13	5.8 \pm 0.5
		10	5.0 \pm 0.8
		11	4.8 \pm 0.3
	10	10	14.9 \pm 1.9
		12	23.2 \pm 1.8
		10	22.6 \pm 1.5
		8	13.5 \pm 1.6
	20	10	31.4 \pm 3.6
		8	25.8 \pm 3.3
		11	43.4 \pm 4.6
		9	43.2 \pm 4.2
2	0	15	2.7 \pm 0.5
		15	3.4 \pm 0.4
	5	15	7.3 \pm 0.9
		15	6.3 \pm 0.7
	10	15	25.2 \pm 1.6
		15	25.9 \pm 2.6
	20	15	32.0 \pm 2.2
		15	29.1 \pm 2.8

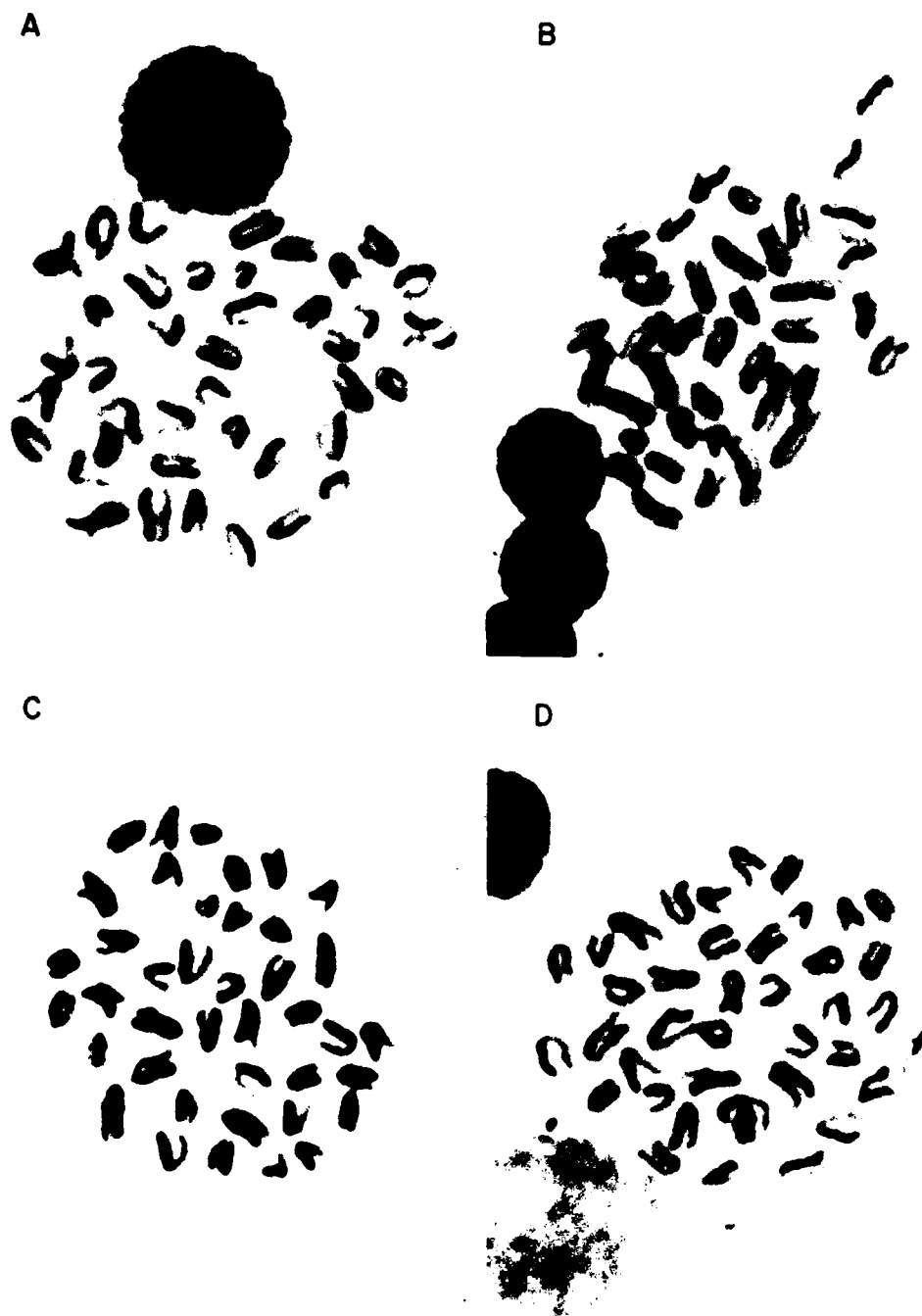


Figure 16. Differentially stained second-division-cycle marrow chromosomes from sham- and RF-irradiated mice. A. Sham exposed; B. 400-MHz exposed; C. 800-MHz exposed; D. 1200-MHz exposed.

TABLE 2. NUMBER OF SCE OBSERVED IN MARROW CHROMOSOMES
OF RFR- AND SHAM-EXPOSED MICE

Each replicate experiment included four RFR- and four sham-exposed animals.
Values in parentheses are number of metaphase cells scored for each animal.

Exposure freq.	Replicate	Mean SCE/cell \pm S.E.M.	
		RFR	Sham
400 MHz	1	4.3 \pm 0.7 (16)	5.2 \pm 0.5 (8)
		4.3 \pm 0.5 (9)	4.5 \pm 0.7 (11)
		6.0 \pm 1.2 (9)	5.5 \pm 0.6 (8)
		5.2 \pm 0.6 (10)	3.9 \pm 0.5 (16)
	2	5.7 \pm 0.7 (10)	5.8 \pm 0.5 (13)
		6.5 \pm 0.9 (12)	3.6 \pm 0.9 (11)
		5.1 \pm 0.9 (12)	5.0 \pm 0.8 (10)
		5.2 \pm 0.7 (12)	4.8 \pm 0.3 (11)
	3	3.4 \pm 0.4 (15)	2.9 \pm 0.5 (15)
		2.8 \pm 0.6 (15)	3.0 \pm 0.3 (15)
		3.0 \pm 0.3 (15)	3.4 \pm 0.4 (15)
		2.8 \pm 0.5 (15)	3.0 \pm 0.3 (15)
800 MHz	1	4.3 \pm 0.7 (10)	5.1 \pm 0.7 (13)
		4.2 \pm 0.5 (11)	3.5 \pm 0.6 (11)
		3.8 \pm 0.5 (9)	5.0 \pm 0.6 (11)
		5.6 \pm 0.8 (13)	3.7 \pm 0.7 (11)
	2	3.8 \pm 0.5 (13)	3.3 \pm 0.6 (17)
		4.0 \pm 0.5 (19)	2.3 \pm 0.4 (18)
		2.2 \pm 0.3 (17)	3.0 \pm 0.5 (16)
		2.2 \pm 0.3 (14)	-- ^a
	3	2.0 \pm 0.3 (15)	2.1 \pm 0.3 (15)
		1.9 \pm 0.3 (15)	1.8 \pm 0.4 (15)
		2.2 \pm 0.4 (15)	2.5 \pm 0.3 (15)
		3.0 \pm 0.7 (15)	2.8 \pm 0.6 (15)
1200 MHz	1	3.6 \pm 0.4 (14)	4.7 \pm 0.6 (24)
		3.4 \pm 0.4 (14)	3.6 \pm 1.0 (11)
		3.9 \pm 0.7 (19)	5.9 \pm 0.6 (17)
		-- ^a	3.4 \pm 0.4 (15)
	2	4.0 \pm 0.5 (18)	4.3 \pm 0.5 (19)
		3.4 \pm 0.4 (19)	5.1 \pm 0.5 (19)
		4.3 \pm 0.5 (22)	2.8 \pm 0.4 (15)
		4.5 \pm 0.4 (20)	3.4 \pm 0.6 (16)

^aCells not scored; no differentiation between the chromatids.

irradiated animals at any of the three exposure frequencies. For each frequency, SCE per cell varied less among animals within each replicate experiment than between animals in different experiments. Therefore, all SCE values for the RFR groups were pooled for each replicate, as were the values for the sham groups. Comparisons of means computed for the pooled data are presented in Table 3. No significant differences were detected between the two treatment groups of any of the replicates, based on two-tailed t-test comparisons. Only in the second replicate of the 400-MHz exposure test did the RFR mean suggest an increase in SCE in response to irradiation. The difference did not prove significant ($P < 0.05$) when further compared using a one-tailed t-test. An earlier RFR-SCE experiment (McRee et al., 1981) exposed mice to 2450-MHz radiation; those results also showed no RFR-induced increases in SCE frequency.

The mean values listed in Table 3 reveal an apparent replication effect. The SCE frequencies in the third 400-MHz replicate and in the second and third 800-MHz replicates are consistently lower than the SCE frequencies of the earlier replicates. We believe this apparent replication effect may reflect differences in the actual amount of BrdUrd given to the animals. We initially prepared the infusion mixtures based on the assumption that the 50 $\mu\text{g}/(\text{g}\cdot\text{h})$ dosage described by Schneider et al. (1978) referred to the absolute amount of BrdUrd. During the latter third of the investigation we had problems achieving satisfactory differential staining between the sister chromatids. In the course of resolving the problems, we discovered that the dosage described by Schneider et al. had been based on the weight of hydrated BrdUrd. We then changed our infusion mixture, calculating dosage on the hydrated rather than absolute weight. The animals in subsequent

TABLE 3. MEAN COMPARISONS OF SCE FREQUENCIES IN MARROW CELLS OF RFR- AND SHAM-EXPOSED MICE

Each mean is a pooled value for the number of cells listed in parentheses.

Exposure freq.	Replicate	Mean SCE/cell \pm S.E.M.		pa
		RFR	Sham	
400 MHz	1	4.9 \pm 0.4 (44)	4.6 \pm 0.3 (43)	0.60
	2	5.6 \pm 0.4 (46)	4.8 \pm 0.3 (45)	0.14
	3	3.0 \pm 0.2 (60)	3.1 \pm 0.2 (60)	0.68
800 MHz	1	4.5 \pm 0.4 (42)	4.4 \pm 0.3 (46)	0.74
	2	3.1 \pm 0.2 (63)	2.8 \pm 0.3 (51)	0.53
	3	2.3 \pm 0.2 (60)	2.3 \pm 0.2 (60)	0.99
1200 MHz	1	3.6 \pm 0.3 (47)	4.5 \pm 0.3 (67)	0.06
	2	4.0 \pm 0.2 (79)	4.0 \pm 0.3 (69)	0.88

^aA two-tailed t-test

experiments therefore received about 2/3 of the absolute level of BrdUrd used in the earlier replicates, a change that seems to be correlated with a drop in the SCE frequency. Schneider et al. showed that SCE frequency did increase as a function of the amount of BrdUrd given to the test animals.

DNA Synthesis: RFR Subjects

The method used to monitor DNA synthesis involved dual labeling with [^{14}C]TdR and [^3H]TdR. Each animal was prelabeled with [^{14}C]TdR, then given the ^3H label, and then sham- or RFR-exposed. This protocol allowed DNA synthesis during RFR treatment to be compared with the preexposure level within the same animal. The percentage of S-phase cells in a given tissue differs between animals, so this protocol eliminated some variances that are due to between-animal differences rather than treatment differences. The protocol is presented in Figure 4.

Table 4 presents results of an experiment designed to test the effectiveness of the dual-labeling procedure for comparing levels of DNA synthesis. Twelve [^{14}C]TdR/[^3H]TdR-labeled mice were treated with different amounts of hydroxyurea, a known inhibitor of semiconservative replication.

TABLE 4. EFFECT OF HYDROXYUREA ON FORMATION OF SPLEEN DNA IN VIVO:
 $^3\text{H}/^{14}\text{C}$ RATIOS USED TO ASSESS RELATIVE LEVELS OF DNA SYNTHESIS

Each value represents one animal. Labeling with [^{14}C]TdR and [^3H]TdR was as described in Technical Approach. Hydroxyurea (0.1 ml of a saline solution) was injected iv 5 min before giving [^3H]TdR. ^{14}C and ^3H radioactivities in the acid-insoluble fraction of the samples were measured and converted to DPM.

Hydroxyurea (mg/kg)	Sample radioactivities		$^3\text{H}/^{14}\text{C}$ ratio	DNA synthesis (% of control)
	^3H DPM	^{14}C DPM		
0	22,000	1,470	15.0	
	36,200	2,190	16.5	
	26,700	1,790	14.9	
			$\bar{y} = 15.5$	100
3	19,400	2,570	7.6	49
	21,600	3,020	7.2	46
	4,600	480	9.6	62
15	4,710	1,860	2.5	16
	4,480	1,620	2.8	18
	1,210	360	3.4	22
150	760	2,050	0.4	3
	530	1,350	0.4	3
	1,610	2,480	0.6	4

Spleens were removed from the animals and analyzed for incorporation of the radioactive precursors into the acid-insoluble fraction. The table shows that administration of hydroxyurea reduced incorporation of [^3H]TdR into DNA relative to the level of [^{14}C]TdR incorporation that preceded the hydroxyurea treatment. More importantly, the $^3\text{H}/^{14}\text{C}$ ratios of all animals receiving the same hydroxyurea dosage were very similar, decreasing as a function of concentration of the inhibitor. These results demonstrate the reliability of the dual-labeling procedure for monitoring DNA synthesis in vivo.

Results of an investigation of DNA synthesis in rodents (Lynch et al., 1970) revealed that [^3H]TdR incorporation into DNA continues linearly for about 30 min and then ceases. Our dual-labeling protocol (Fig. 4) was based on this observation. We chose a 90-min prelabeling to insure completion of [^{14}C]TdR incorporation before giving the second label. The 20 min for the [^3H]TdR pulse represented a compromise between remaining within the period of linear uptake of precursor and maximizing the duration of RFR exposure.

Ratios of ^3H DPM and ^{14}C DPM in the spleen and marrow DNA of animals exposed to the three RFR test frequencies are listed for comparison with their corresponding sham exposed controls in Table 5.

TABLE 5. RELATIVE LEVELS OF DNA SYNTHESIS IN SHAM- AND RFR-EXPOSED MICE

Labeling with [^{14}C]TdR and [^3H]TdR was as described in Technical Approach. Each value is a pooled mean (\pm S.E.M.) of four animals per treatment group and represents the ^3H DPM/ ^{14}C DPM ratio of radioactivities incorporated in spleen or marrow DNA.

Exposure freq.	Replicate	Spleen		Marrow	
		RFR	Sham	RFR	Sham
400 MHz	1	13.7 \pm 0.8	15.4 \pm 1.8	16.0 \pm 1.3	14.9 \pm 2.3 ^a
	2	16.4 \pm 2.0	14.0 \pm 1.2	14.7 \pm 0.9	14.1 \pm 1.1
	3	12.2 \pm 0.9	10.9 \pm 0.9	14.5 \pm 0.5	14.6 \pm 1.8
800 MHz	1	13.4 \pm 1.1	13.2 \pm 1.1	13.1 \pm 0.5 ^a	13.5 \pm 0.5
	2	16.5 \pm 1.8	15.7 \pm 1.0	19.2 \pm 1.0	16.3 \pm 0.9
	3	9.5 \pm 0.6	8.9 \pm 0.8	11.7 \pm 0.4	11.6 \pm 0.3
1200 MHz	1	11.6 \pm 1.7	12.6 \pm 2.1	14.4 \pm 0.7	14.2 \pm 0.9
	2	14.0 \pm 1.0	13.5 \pm 1.0	14.1 \pm 0.7	14.8 \pm 0.5
	3	14.9 \pm 1.9	14.8 \pm 2.1	16.4 \pm 1.3	14.4 \pm 0.5

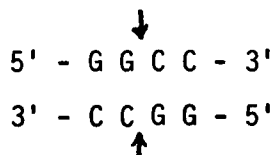
^aMean of three animals only; one sample lost.

The $^3\text{H}/^{14}\text{C}$ ratios summarized in the table reveal no pattern of RFR-induced inhibition of DNA replication. Indeed, quite the opposite may have occurred. The RFR-treatment means of some of the replicates suggest a slightly enhanced level of DNA synthesis in the irradiated animals. This trend is particularly evident for the spleen samples of animals irradiated at 800 MHz. Means computed for the RFR and sham groups were compared within each individual replicate by a one-tailed t-test. Treatment differences were not significant ($P < 0.05$) in any of the replicates including the 800-MHz-irradiated spleen samples. We also used a one-way analysis of variance to test the data of all three replicates at each frequency for a treatment effect. The analysis of variance also revealed no significant differences ($P < 0.05$).

Our results obtained with mice are not in agreement with the RFR effect on DNA synthesis in cultured cells reported by Chang et al. (1980). Those investigators observed a 25% inhibition of DNA synthesis in L1210 cells exposed to a 1000-MHz field at an incident strength of 20 mW/cm^2 . (Not shown here are results we obtained with cultured CHO cells exposed for 60 min at 37.4°C to 1000 MHz at the same field strength used by Chang et al. Results of our tests with the CHO cells revealed no RFR inhibition of DNA synthesis.)

S₁ Hydrolysis of DNA: RFR Effects

The direct tests for RFR-induced denaturation at end regions of DNA required an appropriate substrate, that is, DNA with radioactive moieties at or near exposed ends of the polymer. We envisioned two types of substrates that would fulfill this criterion. One was duplex ^3H -DNA with blunt ends; the other was DNA with single-strand nicks and gaps. The blunt-ended substrate was prepared by HAE III endonuclease treatment which cleaves DNA as shown below:



With this type substrate, having the end G or C bases radioactively labeled was desirable. Thus, the DNA subjected to the HAE III endonuclease treatment was isolated from cultures labeled with $[^3\text{H}]\text{CdR}$. The nicked DNA was prepared by a brief treatment of ^3H -DNA with DNase I. This second type, the nicked DNA, would be seen, for example, at fork regions in replicating DNA where short lengths of nascent DNA, Okazaki fragments, are being formed along an intact template strand. Although the modeling work of Prohofsky and colleagues was based on DNA of the first type (Kohli et al., 1981), the second type is perhaps more likely to be encountered in the cell.

An initial experiment was performed to test the activity of the nuclease with different types of substrates. The ^3H -DNA used in that experiment was isolated from subconfluent cultures of CHO-K₁ cells ($\sim 3 \times 10^6$ cells/100-mm dish at harvest) labeled overnight with $[^3\text{H}]\text{TdR}$ at a concentration of $1 \mu\text{Ci/ml}$ culture medium. Approximately two-thirds of the DNA recovered from these cells was treated with HAE III restriction endonuclease in the reaction mixture described by Blakeley et al. (1977). The remaining third, referred to

as whole DNA, was used without further treatment. A portion of the HAE III digest was heat denatured. The three different preparations (whole DNA, HAE III duplex fragments, and denatured HAE III fragments) were then treated with S_1 nuclease. Results, presented in Table 6, indicate that the nuclease was definitely single-strand-specific as evidenced by the essentially complete hydrolysis of denatured substrate compared with only 1% hydrolysis of the whole duplex DNA substrate. Apparently, some single-stranded regions were created during the HAE III treatment, as indicated by the partial hydrolysis of the HAE III fragments incubated with the high level of S_1 nuclease. We speculated that this problem may have been due to partial strand separation caused by an inadequate concentration of salt in the HAE III reaction mixture used, the mixture described by Blakeley et al. (1977). In subsequent experiments we added NaCl to a concentration of 0.15 M to avert this problem.

TABLE 6. TEST OF DNA TYPE USED AS SUBSTRATE FOR S_1 HYDROLYSIS

Each reaction vessel contained ~30 μ g of ^3H -DNA (~10,000 CPM) in a volume of 0.5 ml. Incubation was for 30 min.

Type of DNA substrate	S_1 Nuclease (μ g)	Radioactivity (CPM)		% Hydrolysis
		Acid-sol. frac.	Acid-insol. frac.	
Whole duplex	---	52	7,870	0.6
	0.6	102	9,680	1.0
	6	127	12,400	1.0
Hae III ^a duplex fragments	---	41	10,400	0.3
	0.6	712	10,900	6.1
	6	1,500	6,620	18.5
Heat-denatured HAE III ^a fragments	---	30	8,030	0.3
	0.6	7,510	337	95.7
	6	8,180	154	98.1

^aFor HAE III digestion, 100 μ g of DNA was incubated for 30 min at 37°C with 200 units of HAE III endonuclease in the reaction mixture described by Blakeley et al. (1977).

The effect of RFR on S_1 nuclease catalyzed hydrolysis of DNA was then tested using five types of DNA substrates. The substrates, type I to V (listed in Table 7), were prepared from CHO-K1 cultures ($\sim 2 \times 10^6$ cells/100-mm dish at harvest) labeled overnight either with [^3H]TdR at a concentration of 25 $\mu\text{Ci/ml}$ or with [^3H]CdR at a concentration of 6.25 $\mu\text{Ci/ml}$. DNA isolated from the [^3H]TdR-labeled cultures was used without further treatment (substrate type I) or was subjected to treatment with DNase I (substrate type II) or heat denaturation (substrate type IV). DNA isolated from the [^3H]CdR-labeled cells was either treated with HAE III endonuclease (substrate type III) or heat denatured (substrate type V). Preparation of the type II substrate involved preincubation of 33 μg of the [^3H]TdR-labeled DNA at 37.4°C in a reaction mixture (0.3 ml) containing 0.15 M NaCl, 10 mM MgSO_4 , and 0.1 M sodium acetate, pH 5.0. DNase I (0.4 unit) was then added and the incubation continued for 30 s, whereupon 5 μg of actin, a known inhibitor of DNase I (Lazarides and Lindberg, 1974), was added. The brief DNase I treatment resulted in a noticeable decrease in viscosity of the DNA. The amount of DNase I needed for this treatment was determined by preliminary experimentation (results not shown). The blunt-ended type III substrate was prepared by a 30-min incubation of 30.5 μg of [^3H]CdR-labeled DNA with 75 units of HAE III endonuclease in the mixture of Blakeley et al. (1977), with NaCl added to 0.15 M.

The different levels of S_1 hydrolysis of these substrates as a result of RFR exposure and control incubation are summarized in Table 7. As expected, the DNase I treated DNA (substrate II) was the most susceptible to the action of the nuclease. Whole DNA was included in the test as a control substrate, that is, a substrate expected to be relatively resistant to the nuclease. Interestingly, our whole DNA preparation was more susceptible to the nuclease than was the blunt-ended type III substrate. This may reflect a somewhat greater degree of mechanical degradation of the [^3H]TdR-labeled DNA than the [^3H]CdR-labeled DNA occurring during isolation from the cell cultures. Both of the single-stranded heat-denatured substrates (types IV and V) were almost completely hydrolyzed by the S_1 nuclease. This indicates that the substrate concentration was not saturating. An overview of the data in Table 7 reveals that the extent of hydrolysis occurring is slightly, but consistently, higher in the RF-irradiated samples than the corresponding control samples. This was true not only with all three of the duplex substrates used, but also at all three of the test exposure frequencies. Such differences could occur as artifacts due to slight differences in the reaction-mixture temperatures that influenced the reaction kinetics. Temperatures of the RFR and sham tubes monitored during the course of the 60-min S_1 nuclease reaction were found, however, to be essentially the same. These measurements were performed with two Vitek 101 monitors, with the probes inserted in capillary tubes filled with S_1 reaction mixture (minus DNA). One tube with probe was placed in the water bath and the other was placed in the RFR enclosure, parallel to the E-field and approximately 2 cm from the experimental tubes. Temperatures recorded by the monitors were $37.4 \pm 0.1^\circ\text{C}$ for the water bath and $37.4 \pm 0.3^\circ\text{C}$ for the irradiated tube. To the extent that our temperature monitors are accurate (as they have proven to be in numerous other tests), we believe that the differences between the RFR and sham samples shown in Table 7 are not due to temperature differences.

Several questions may be addressed if the apparent RFR-enhancement of S₁ nuclease hydrolysis of ³H-DNA evidenced by the results listed in Table 7 is real. First, why was there no manifestation of the phenomenon in vivo? One reason may be that intact chromatin does not undergo the same vibrational responses that isolated DNA does. Second, why did the enhancement of hydrolysis occur at all three exposure frequencies rather than at one specific frequency? For this, we cannot suggest an explanation. The experiment is by no means definitive, but it does suggest problem areas for further exploration of RFR effects on biologic systems.

TABLE 7. EFFECT OF RFR EXPOSURE ON HYDROLYSIS OF ³H-DNA BY S₁ NUCLEASE

Each capillary-tube reaction vessel contained 6 µg of S₁ nuclease plus either 6.2 µg (1.23 x 10⁶ CPM) of [³H]TdR-labeled DNA (substrate I, II, or IV) or 5.7 µg (2.94 x 10⁵ CPM) of [³H]CdR-labeled DNA (substrate III or V). Irradiated samples were exposed to incident field strengths of 16 mW/cm² (400 MHz), 12.5 mW/cm² (800 MHz), or 5.3 mW/cm² (1200 MHz), and an air temperature of 37.4°C. Sham (control) tubes were incubated in a 37.4°C water bath. Incubation was for 60 min. Each value is the mean ± S.D. of two tubes.

Exposure freq.	Substrate type	RFR		Sham	
		Acid-sol CPM (10 ⁻³)	% hydrolysis	Acid-sol CPM (10 ⁻³)	% hydrolysis
400 MHz	I ^a	36.7 ± 0.9	3.0	35.0 ± 2.5	2.8
	II ^b	161.7 ± 0.7	13.1	140.7 ± 0.3	11.4
	III ^c	6.8 ± 0.1	2.3	5.6 ± 0.1	1.9
800 MHz	I	33.9 ± 0.2	2.7	26.6 ± 0.5	2.2
	II	133.0 ± 2.3	10.8	127.7 ± 0.9	10.4
	III	4.1 ± 0.1	1.4	4.1 ± 0.6	1.4
1200 MHz	I	45.8 ± 4.3	3.7	34.5 ± 3.0	2.8
	II	296.5 ± 7.8	24.1	254.2 ± 6.1	20.7
	III	2.9 ± 0.2	1.0	2.7 ± 0.1	1.0
---	IV ^d			1,155.0 ± 6.2	94
	V ^d			304.7 ± 0.8	103

^aSubstrate I was whole (untreated) duplex DNA.

^bSubstrate II was DNase I-treated duplex DNA.

^cSubstrate III was duplex DNA treated with HAE III restriction endonuclease.

^dDNA substrates IV and V were both heat denatured.

CONCLUSIONS

Two of the three experimental approaches of this investigation yielded results indicating no decrease in either the stability or the rate of replication of DNA in mice exposed to RFR at incident field strengths equivalent to an SAR of 4 W/kg in the large mouse. The level of DNA synthesis was not reduced in either the spleen or the bone marrow of mice irradiated at any of the three test frequencies. RFR exposure was also without effect on the frequency of SCE in bone marrow cells, used here as one index of chromosome stability. The third approach, also a test of DNA stability, yielded results suggestive of a possible RFR-induced melting of hydrogen bonds at nicked regions of duplex DNA. This was evidenced by slightly increased susceptibility of DNase I treated, RF-irradiated DNA to a single-strand-specific nuclease. The absence of any observable in vivo counterpart suggests that the magnitude of the latter effect was insufficient for physiologic significance.

ACKNOWLEDGMENTS

Skilled technical assistance was provided by Ms. Cornelia Myers and Ms. Sharon Powell.

REFERENCES

- Ando, T. A nuclease specific for heat-denatured DNA isolated from a product of Aspergillus oryzae. *Biochim Biophys Acta* 114:158-168 (1966).
- Blakeley, R.W., J.B. Dodgson, I.F. Nes, and R.D. Wells. Duplex regions in single-stranded ϕ X174 DNA are cleaved by a restriction endonuclease from Haemophilus aegyptius. *J Biol Chem* 252:7300-7306 (1977).
- Brown, R.F., S.V. Marshall, and C.W. Hughes. Effect of radiofrequency radiation (RFR) on excision-type DNA repair in vivo. University of Missouri-Rolla, Final project report, Contract No. F33615-80-C-0613 with USAF School of Aerospace Medicine, Brooks AFB, Texas, 1981.
- Brown, R.F., T. Umeda, S. Takai, and I. Lieberman. Effect of inhibitors of protein synthesis on DNA formation in liver. *Biochim Biophys Acta* 209:49-53 (1970).
- Carrano, A.V., L.H. Thompson, P.A. Lindl, and J.L. Minkler. Sister chromatid exchange as an indicator of mutagenesis. *Nature* 271:551-553 (1978).
- Chang, B.K., A.T. Huang, and W.T. Joines. Inhibition of DNA synthesis and enhancement of the uptake and action of methotrexate by low-power-density microwave radiation in L1210 leukemia cells. *Cancer Res* 40:1002-1005 (1980).
- Collins, J.M. Deoxyribonucleic acid structure in human diploid fibroblasts stimulated to proliferate. *J Biol Chem* 252:141-147 (1977).
- Durney, C.H., M.F. Iskander, H. Massoudi, S.J. Allen, and J.C. Mitchell. Radiofrequency radiation dosimetry handbook, 3d edition. SAM-TR-80-32, Aug 1980.
- Durney, C.H., C.C. Johnson, P.W. Barber, H. Massoudi, M.F. Iskander, J.L. Lords, D.K. Ryser, S.J. Allen, and J.C. Mitchell. Radiofrequency radiation dosimetry handbook, 2d edition. SAM-TR-78-22, May 1978.
- Gross-Bellard, M., P. Oudet, and P. Chambon. Isolation of high molecular-weight DNA from mammalian cells. *Eur J Biochem* 36:32-38 (1973).
- Hanawalt, P.C., P.K. Cooper, A.K. Ganesan, and C.A. Smith. DNA repair bacteria and mammalian cells. *Annu Rev Biochem* 48:783-836 (1979).
- Huberman, J.A., and H. Horwitz. Discontinuous DNA synthesis in mammalian cells. *Cold Spring Harbor Symposium. Quant Biol* 38:233-238 (1973).
- Kohli, M., W.N. Mei, E.W. Prohowsky, and L.L. VanZandt. Calculated microwave absorption of double-helical B-conformation poly(dG).poly(dC). *Biopolymers* 20:853-864 (1981).
- Lampert, F., G.F. Bahr, and E. DuPraw. Ultrastructure of a Burkitt's lymphoma marker chromosome as investigated by quantitative electron microscopy. *Cancer* 24:367-376 (1969).

- Lazarides, E., and U. Lindberg. Actin is the naturally occurring inhibitor of deoxyribonuclease I. *Proc. Nat Acad Sci USA* 71:4742-4746 (1974).
- Lehmann, A.R. Postreplication repair of DNA in mammalian cells. *Life Sci* 15:2005-2016 (1974).
- Livingston, G.K., and L.A. Dethlefsen. Effects of hyperthermia and X irradiation on sister chromatid exchange (SCE) frequency in Chinese hamster ovary (CHO) cells. *Radiat Res* 77:512-520 (1979).
- Lubs, H.A., W.H. McKenzie, S.R. Patil, and S. Merrick. New staining methods for chromosomes. *Methods Cell Biol* 6:345-380 (1973).
- Lynch, W.E., R.F. Brown, T. Umeda, S.R. Langreth, and I. Lieberman. Synthesis of deoxyribonucleic acid by isolated liver nuclei. *J Biol Chem* 245:3911-3916 (1970).
- McRee, D.I., G. MacNichols, and G.K. Livingston. Incidence of sister chromatid exchange in bone marrow cells of the mouse following microwave exposure. *Radiat Res* 85:340-348 (1981).
- Mei, W.N., M. Kohli, E.W. Prohofsky, and L.L. VanZandt. Acoustic modes and nonbonded interactions of the double helix. *Biopolymers* 20:833-852 (1981).
- Minkler, J., D. Steka, and A.V. Carrano. An ultraviolet light source for consistent differential staining of sister chromatids. *Stain Technol* 53:359-360 (1978).
- Perry, P., and H.J. Evans. Cytological detection of mutagen-carcinogen exposure by sister chromatid exchange. *Nature* 258:121-125 (1975).
- Perry, P., and S. Wolff. New Giemsa method for the differential staining of sister chromatids. *Nature* 251:156-158 (1974).
- Putnam, B.F., L.L. VanZandt, E.W. Prohofsky, and W.N. Mei. Resonant and localized breathing modes in terminal regions of the DNA double helix. *Biophys J* 35:271-287 (1981).
- Schneider, E.L., Y. Nakanishi, J. Lewis, and H. Sternberg. Simultaneous examination of sister chromatid exchanges and cell replication kinetics in tumor and normal cell in vivo. *Cancer Res* 41:4973-4975 (1981).
- Schneider, E.L., R.R. Tice, and D. Kram. Bromodeoxyuridine differential chromatid staining technique: A new approach to examining sister chromatid exchange and cell replication kinetics. *Methods Cell Biol* 20:379-409 (1978).
- Schreck, R.R., I.J. Paika, and S.A. Latt. In vivo induction of sister chromatid exchanges in liver and marrow cells by drugs requiring metabolic activation. *Mutation Res* 64:315-328 (1979).
- Vogt, V.M. Purification and further properties of single-strand-specific nuclease from Aspergillus oryzae. *Eur J Biochem* 33:192-200 (1973).

